Environ Earth Sci
DOI 10.1007/s12665-014-3226-5

ORIGINAL ARTICLE

Hydrochemistry to delineate groundwater flow conditions in the Mogher Al Mer area (Damascus Basin, Southwestern Syria)

N. M. Asmael · F. Huneau · E. Garel · H. Celle-Jeanton · P. Le Coustumer · A. Dupuy

Received: 11 February 2013 / Accepted: 20 March 2014
© Springer-Verlag Berlin Heidelberg 2014

Abstract The hydrochemistry of groundwater from the Mogher Al Mer area, located in southwestern Syria, has been used as a tool to identify and assess the hydrogeological systems and associated conditions. In this arid region of Syria, groundwater is considered as the main source of water supply for both drinking and irrigation purposes. The detailed description of hydrogeochemical conditions, including major ions, physico-chemical and in situ field parameters, has underlined the very complex variability of the stratigraphic sequences and hence the numerous hydrogeological units within the study area. On the one hand, groundwater chemical signature is found to be mainly controlled by the water–rock interaction processes in the mountainous western part of the study area. On the other hand, anthropogenic influences are observed in the eastern plain. In terms of recharge mechanisms, the region can be considered as a part of a main intermediate or even regional flow system instead of a local one.

Keywords Aquifer · Groundwater · Hydrochemistry · Arid region · Syria

N. M. Asmael
Department of Geology, Faculty of Sciences, University of Damascus, P.O. Box 32022, Damascus, Syria

N. M. Asmael · P. Le Coustumer · A. Dupuy
EA 4592 Géoressources & Environnement, Université de Bordeaux, 1 allée F. Daguin, 33607 Pessac, France

F. Huneau (✉) · E. Garel
Laboratoire d'Hydrogéologie, Faculté des Sciences et Techniques, Université de Corse Pascal Paoli, Campus Grimaldi, BP 52, 20250 Corte, France
e-mail: huneau@univ-corse.fr

F. Huneau · E. Garel
CNRS, UMR 6134, SPE, 20250 Corte, France

H. Celle-Jeanton
Laboratoire Magmas et Volcans, Clermont Université, Université Blaise Pascal, BP 10448, 63038 Clermont-Ferrand, France

H. Celle-Jeanton
CNRS, UMR 6524, LMV, 63038 Clermont-Ferrand, France

H. Celle-Jeanton
IRD, R 163, LMV, 63038 Clermont-Ferrand, France

A. Dupuy
ENSEGID-IPB, 1 allée F. Daguin, 33607 Pessac, France

Introduction

In the former days, the Barada and Awaj Rivers, mainly fed by karst springs (Wolfart 1964), were considered as a vital socioeconomic resource, sustaining the Ghouta Oasis and agricultural activities in the Damascus Basin (Barada and Awaj Basin) (INECO 2009).

Due to the decrease in surface water supplies in the study area, groundwater remains the only option to supplement the ever-growing demand for water to meet the requirement of human activities (Al-Charideh 2011, 2012a, b). Therefore, additional threat is put on all fresh groundwater resources. The protection and management sustainable of groundwater resources is a priority objective in both industrialized and developing countries (European Commission 1995; Barbieri et al. 2005). Groundwater management in Syria is an issue of great concern to water policy makers, planners, and legislators, with respect to pollution and resources sustainability (FAO 1993; Angelakis 2000).

Published online: 13 April 2014

Consumption rates greater than recharge rates are common in the last 20 years in most regions of Syria. Consequently, groundwater levels have started to decrease dramatically and negative water balance has been detected. Several springs have dried up and a large number of rivers have become seasonal or have been converted to wastewater canals (Al-Charideh and Abou-Zakhem 2009; Meslmani and Wardeh 2010). From a holistic perspective, a conceptual approach that encompasses human pressures must recognize the hydrogeological heterogeneity caused by the complexity of the geological structure. Also the potential contributions of distinct recharge areas have to be identified once groundwater withdrawal has begun (Mahlknecht et al. 2006; Palmer et al. 2007; Li et al. 2008; Folch et al. 2011).

The characterization of the flow conditions within the local aquifers is an important step towards a better management of water resources. Hydrochemistry can provide an important information and independent method for identifying recharge areas and delineating preferential flow paths. Groundwater carries chemical signatures of recharge precipitation and interactions along flow paths with aquifers rocks as well as anthropogenic activities (Rakhmatullaev et al. 2010, 2012; Huneau et al. 2011).

Groundwater in the Mogher Al Mer area is the main source of water supply for small population centres as well as for private use in agriculture and cattle supply. However, the processes (natural or anthropogenic) controlling the chemistry and quality of groundwater in this area is not yet well understood. Therefore, the main objectives of the present study are to (1) evaluate relevant rock–water interactions that influence water quality in the study area within the framework of its complex geology and morphology, (2) determine predominant water type based on their chemical compositions and ionic ratios, (3) interpret the groundwater flow system conditions to update and improve the knowledge on the groundwater flow behaviour.

General setting of the study area

The Damascus Basin occupies the southwestern part of the Syrian Arab Republic (SAR).The climate of SAR is characterized by warm dry summers and cool rainy winters. SAR has scare water resources with more than 60 % of the country receiving less than 250 mm/year of rainfall (Mourad and Berndtsson 2011). Annual precipitation in the Damascus Basin varies in the range of 86–900 mm/year and this basin is classified into four climatic zones: hot desert, arid, semiarid, and moderate (RDAWSA 2006).

A high variation in the air temperature is observed between winter and summer. Temperatures can drop down below freezing point at high altitudes (1,500–2,000 m) in winter and can reach 42 °C during summer. The relative humidity is usually about 24–50 % during summer (July and August) and may reach up to 60–70 % during winter (January and February). The annual average potential evaporation varies between 1,500 mm/year in the flatlands and 1,100 mm/year in the mountainous areas. Evapotranspiration in the mountainous area varies between 300 and 400 mm/year and it is close to precipitation in the flatland area (Selkhozpromexport 1986; Kattan 1997).

Mogher Al Mer and its surrounding areas (Fig. 1) cover an area of approximately 400 km^2. This region is considered as a main recharge area of Awaj River which is the main watercourse in this area. The annual average discharge of Awaj River is 4.7 m^3/s (MOI 2005). Topographically, the area is characterized by mountains in the west and northwest with sharp deep valleys in between, and by a flat area in the east and southeast. The relief varies between 800 and 1,800 m.a.s.l.

Geological and hydrogeological setting

Geology

The main formations outcropping in the study area range from the Middle Jurassic up to the Quaternary period. The major Jurassic deposits are found in the Mt Hermon (western and northwestern parts), whereas the plain areas are characterized by outcroppings of the Paleogene, Neogene, and Quaternary deposits. The Cretaceous formation is exposed in a small part southwest of the study area. The Paleogene formation is found in the southern part. The thickness of Paleogene is about 1,500 m and is composed of limestone characterized by nummulites and interbedded with marl layers and clayey marls in the upper part of the Eocene. The Neogene formation is outcropping in the central and eastern parts of the study area with a thickness of about 500 m. The dark colored Miocene basalts, which are characterized by fractures filled with calcite, are found locally beneath the conglomerates of Pliocene age. The Quaternary deposits are mainly found in the plain area around the Awaj River. Its thickness varies between 1 and 10 m. Figure 2 displays three cross sections showing subsurface lithology as well as the major structures within the study area and the logs of wells penetrating Neogene, Palaeogene, Cretaceous, and Jurassic formations.

In terms of tectonic, the area is strongly affected by faulting and folding resulting in several folded structures such as Mt. Anti-Lebanon (up to 2,466 m) and Mt. Hermon (2,814 m) (Dubertret 1932; Ponikarov 1967; Selkhozpromexport 1986; La-Moreaux et al. 1989; Kattan 2006). Generally, most strata from Jurassic to Cretaceous age are

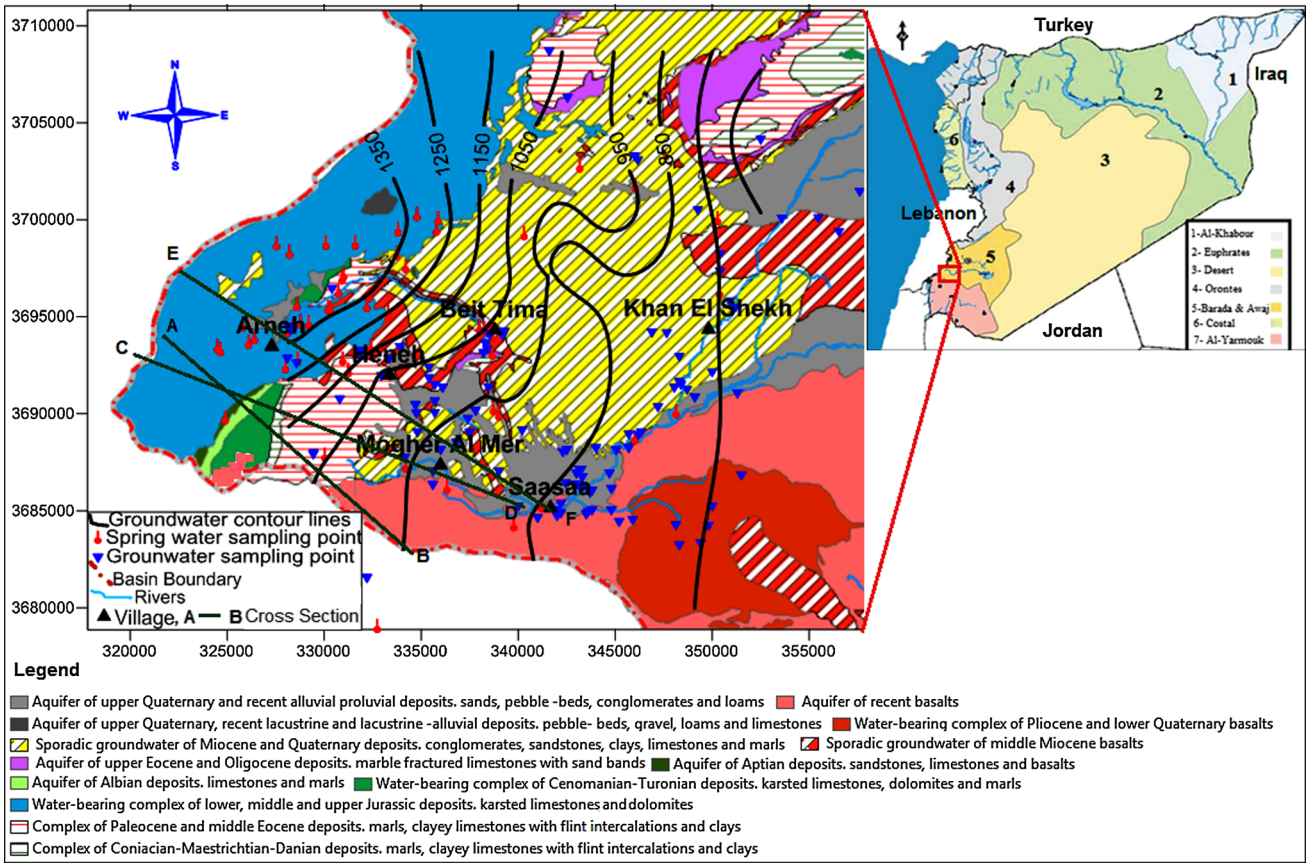

Fig. 1 Map of Syria divided into seven basins with the location of study area in the Barada and Awaj Basin. The locations of sampling sites, groundwater equipotential contours, and three geological cross sections presented in Fig. 2 are shown on hydrogeological map of the study area

dipping in the southeast direction to the east Mt. Hermon. The tectonic activities, mainly fault zones, together with karstic features, seem to play a significant role in this area in terms of increasing infiltration coefficient and controlling groundwater flow behaviour, and recharge/discharge mechanisms (Burdon and Safadi 1964).

Hydrogeology

The aquifers in the study area can be classified into karstic and porous aquifers.

The karstic aquifers consist of limestones and dolomites, which upon dissolution along faults and fractures create a secondary porosity. Such aquifers belong to the Jurassic, the Cenomanian–Turonian, and the Upper Eocene units (Al-Charideh 2012a). Porous formations consist of unconsolidated or semi-consolidated sediments, such as the Pliocene conglomerate units and the Quaternary aquifer. The basalts, if not intensely fractured, can be considered to a certain extent as an aquiclude (Kattan 1997, 2006).

Figure 1 shows the hydrogeological map of the study area with major aquifers. The major hydrogeological units in the study area are classified and described below (Selkhozpromexport 1986):

Jurassic unit

The karstic limestone layer containing gypsum infilling (about 2,000 m thick) interbedded with dolomite, dolomitic limestone, and marls layers forms this unit. The hydraulic conductivity varies between 2 and 99.3 m/day, and the transmissivity is about 3,085 m^2/day (RDAWSA 2006).

Cretaceous unit

The limestone, dolomitic limestone, and crystalline dolomite interbedded with argillaceous limestone, marl, and sandstone formations compose the aquifer member of this unit (400–1,000 m). This unit together with the Jurassic unit represents the most important water-bearing system in the Damascus Basin and even in the SAR in terms of storage capacity and discharge of springs (JICA 2001). The hydraulic conductivity is up to 80 m/day and transmissivity varies between 12 and 7,435 m^2/day (La-Moreaux et al. 1989).

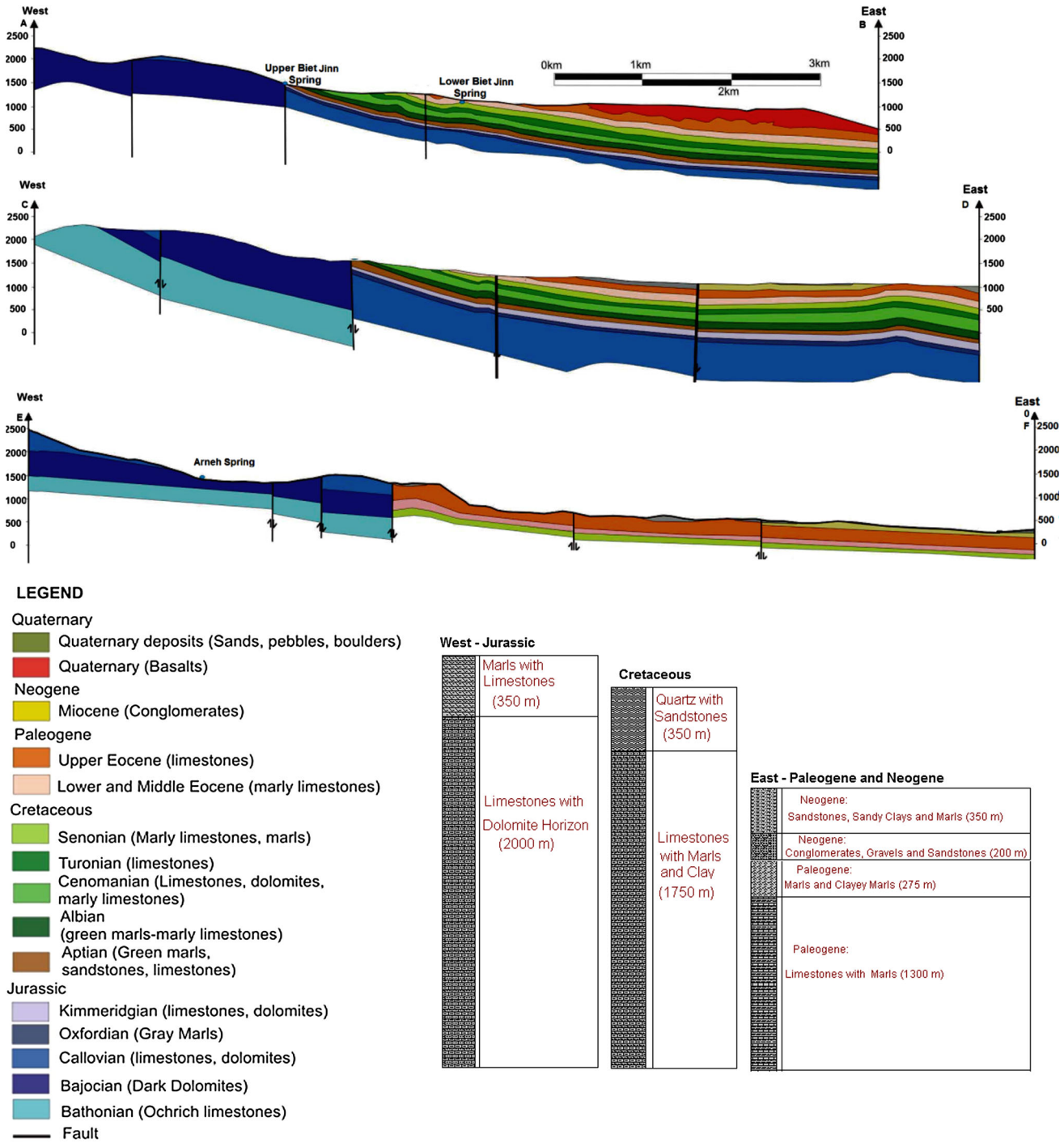

Fig. 2 Three geological cross sections showing subsurface lithology as well as the major structure within the study area and the logs of wells tapping Neogene, Paleogene, Cretaceous, and Jurassic formations

Sedimentary Mio–Quaternary aquifer

The rocks of this complex (140–630 m thick) are widespread on the foothill of Mt. Hermon and in the plain area. They consist of gravels and conglomerates interbedded with clay, sandstone, and limestone. As clay content increases and/or aquifer thickness decreases, the transmissivity value can drop down from 756 to 0.05 m^2/day.

Volcanic middle Miocene aquifer

The Basaltic aquifer (500 m) consists of fissured basalts associated with thin beds and lenses of sand and sandstone. This aquifer overlays the Neogene conglomerates. The transmissivity of this aquifer is about 30–60 m^2/day. Almost all the springs emerging from the basalts aquifer originate from deeper aquifers, such as the Neogene conglomerates or other related aquifers.

Groundwater contour map

Based on available water level data on 33 groundwater monitoring points obtained from Ministry of Irrigation of Syria, a preliminary potentiometric map was constructed for November 2006 as shown in Fig. 1. The interpretation of equipotential contours indicates that the general groundwater flow is organized towards the east direction. Minor flow direction is also recognized from northwestern to southeastern where several springs characterized by relatively high discharge rates are emerging. A stepper hydraulic gradient is observed in the western and northern mountainous parts, where the karsts and faults are more developed.

Sampling, analysis, and database preparation

A total of 107 water samples from springs and wells (Fig. 1) were collected during the fieldwork campaign in November and December 2006. Wells depths range between 35 and 160 m and are owned by the Ministry of Irrigation and farmers. Samples were collected in polyethylene bottles, which were rinsed twice with sample water. Two bottles of each water point were collected. One bottle was filtered (0.45 μm) and acidified with two drops of nitric acid, (HNO_3) for cations determination.

Field parameters such as electrical conductivity (EC), pH, and alkalinity (HCO_3^-) were measured onsite. Within 30 days of sampling, all samples were analysed in the UNESCO-IHE Institute laboratory in The Netherlands. Cation concentrations were measured using an Absorption Spectrophotometer (AAS), whereas the anions were measured with Dionex Ion Chromatograph (DIOEX ICC-1000). Silica (as SiO_2) was measured using HACH colorimeter. In addition, the database was completed with other available related data from different sources (RDAWSA 2006; Selkhozpromexport 1986). Using PHREEQC (Parkhurst and Appelo 1999), different calculations were performed to determine water types according to Stuyfzand classification (Stuyfzand 1989), and the saturation indices of a selection of minerals and the partial pressure of carbon dioxide. Field parameters and majors ions for the different sampling points are displayed in Table 1.

Results and discussion

To protect valuable water resources effectively and to predict any change in groundwater environments, it is necessary to understand the hydrochemical characteristics of the groundwater and its evolution under natural water circulation processes (Lawrence et al. 2000; Guendouz et al. 2003; Wen et al. 2005; Ma et al. 2005; Edmunds et al. 2006; Ma and Edmunds 2006; Jianhua et al. 2009). The motion of groundwater along its flow paths generally increases the concentration of the chemical species (Domenico and Schwartz 1990; Freeze and Cherry 1979; Kortatsi 2007; Aghazadeh and Mogaddam 2011).

Calcite, dolomite, and gypsum dissolution

The dissolution of limestones and dolomites is a dominant mineralization process for groundwater of carbonate systems. In many cases, the dissolution of gypsum has also a very important role (Flakova 1998). The most important factor determining the solubility of minerals is the abundance of carbon dioxide in the system. The process of calcite and dolomite dissolution takes place under conditions of open and closed systems, depending on the CO_2 pressure. Figure 3 shows the pure calcite and dolomite dissolution under both open and closed system dissolution as a function of CO_2 supply determined by PHREEQC (Parkhurst and Appelo 1999). The relationship between measured pH and calculated pCO_2 in the water samples is also shown on this figure. In the closed system, CO_2 is decreasing along the groundwater flow path. On the other hand, it remains constant in the open system (Appelo and Postma 2005). The ranges of calculated pCO_2 as a function of pH in the water samples comparing with those values of open and close system dissolution indicated that open system dissolution is prevailing in the study area.

During the contact between infiltrating water and limestones, dolomites and gypsum, congruent or incongruent dissolution of carbonate minerals can occur. Mineral equilibrium calculations for groundwater are useful in predicting the presence of reactive minerals in the groundwater system and estimating mineral reactivity (Deutsch 1997; Jianhua et al. 2009).

Since open system dissolution of carbonates is suspected, bicarbonate, calcium, and magnesium concentrations have been plotted as a function of calculated pCO_2 together with the pure calcite and dolomite dissolution determined with PHREEQC (Fig. 4a). The PHREEQC lines and the scatter plot determine the dissolution state of the carbonate system. Distinctly, this graph shows different sources of calcium in water samples because most of the samples are plotted above PHREEQC lines. In contrast, bicarbonate and magnesium for most samples are situated below those lines.

Table 1 List of sampling sites and chemical composition of water samples collected during November and December 2006 and the historical data based on Selkhozpromexport study performed on 1986

Name	Location	Date	Type	EC (μS/cm)	pH (−)	T (°C)	Na^+ (mg/L)	K^+ (mg/L)	Mg^{2+} (mg/L)	Ca^{2+} (mg/L)	Cl^- (mg/L)	HCO_3^- (mg/L)	SO_4^{2-} (mg/L)	NO_3^- (mg/L)	SiO_2 (mg/L)	σ (%)
Artesian well	Arneh	Dec-06	W	660	7.5	14.4	4.9	0	20	120	5.7	238	196.5	4	6.6	−2.6
Drink well	Harfa	Nov-06	W	462	7.3	17.8	15.6	13.8	4	67	24.2	162.3	9.6	49.7	14.4	4.0
Artesian well	Harfa	Nov-06	W	431	7.8	15.5	10.9	5.7	23	31	7.7	244	0.7	0.4	10.2	−2.2
well6	Heneh	Nov-06	W	570	7.6	18.7	20.7	1	25	59	29.1	223.3	63	25.1	22.6	−2.3
well1	Heneh	Nov-06	W	443	7.3	17.4	9.2	0	10	72	14.1	231.8	9.5	15.4	26.6	1.9
well5	Heneh	Nov-06	W	708	7.2	18.4	22.3	2	16	101	36.5	247.7	42.6	66	18.8	2.4
MJ Alshekh	Heneh	Nov-06	W	681	7.3	13.4	20.3	1.1	14	106	43.1	253.8	47	59.8	15.6	0.1
well1	Kleaa	Dec-06	W	530	7.2	17.2	16.4	3.7	10	87	24	264.7	14.7	22	14	2.6
well2	Kleaa	Dec-06	W	532	7.3	16.9	11.9	1.7	11	94	35.6	249	8	24.6	11.4	4.4
well3	Kleaa	Dec-06	W	685	7.4	17.5	30.3	2.7	15	98	47	234.2	69.1	22.4	13	4.0
well1	Remeh	Dec-06	W	350	7.5	13.1	3.3	0	3	65	5.9	207.4	5.2	9.6	5.6	−2.7
well1	Dorbol	Nov-06	W	480	7.5	13.6	7.8	0	6	86	17.2	253.8	11.7	11.4	24.2	0.5
well2	Dorbol	Nov-06	W	430	7.3	14.8	5.8	0	5	86	7.4	261	5.4	5.3	22	2.9
well1	Drosha	Dec-06	W	424	7.4	18.4	7.5	1.4	8	75	12	211.1	15.7	17.5	10.2	4.0
well2	Heneh	Nov-06	W	842	7	18.2	42.8	15.5	21	106	29.3	414	59	35.2	31.6	−0.7
well1	Knaker	Dec-06	W	418	7.7	17.4	22.6	1.7	12	53	22	196.4	19.6	15.8	15	1.8
well2	Knaker	Dec-06	W	386	7.6	18.3	12.2	1.5	12	58	16.7	197.6	11.6	15	12.8	3.1
well3	Knaker	Dec-06	W	378	7.4	16.1	13.3	1.8	8	56	16.5	183	12.5	13.6	13.2	1.7
well4	Knaker	Dec-06	W	387	7.5	17.1	14.8	1.8	9	63	14	198.9	8.9	21.1	12.8	4.6
well1	Saasaa	Nov-06	W	685	7.3	16.6	14	2.3	11	100	103.6	213.5	5.7	22.8	12.6	−2.6
well2	Saasaa	Dec-06	W	633	7.5	17.2	17.2	2	11	99	35.4	294	43	18	12.8	−2.7
well3	Saasaa	Dec-06	W	625	7.2	17.1	15.6	2	12	108	30.5	274.5	59.6	16.3	13	1.8
well4	Saasaa	Dec-06	W	542	7.3	15.7	14	1.8	8	87	34.5	262.3	12.1	34.8	11	−3.8
well5	saasaa	Dec-06	W	515	7.2	15.1	11.7	1.5	9	90	21.5	280.6	21.2	27.3	11.8	−2.7
well6	Saasaa	Dec-06	W	551	7.2	16.1	12.7	1.6	9	97	16.7	283	7.1	37.4	12.4	2.7
well7	Saasaa	Dec-06	W	350	7.6	17.9	17.2	1.7	5	53	13	190.3	6.3	6.6	11	1.7
well8	Saasaa	Dec-06	W	430	7.4	18.6	13	1.9	7	58	34.6	48.8	5.2	154.4	11.6	−3.4
well9	Saasaa	Dec-06	W	434	7.7	18.9	27.7	2.4	7	50	36.6	163.5	10.6	30.4	13	−1.0
well10	Saasaa	Dec-06	W	385	7.5	17.1	13.9	1.9	6	55	19.1	176.9	4.9	9.2	10.6	2.7
well12	Saasaa	Dec-06	W	443	7.7	17.1	29.6	2.3	6	65	29.9	219.6	9.5	6.6	11.4	3.5
well14	Saasaa	Dec-06	W	410	7.4	16.6	10.1	2.3	7	66	19.8	194	7	14.5	11.6	3.0
well15	Saasaa	Dec-06	W	510	7.5	16.6	17.6	2.1	10	70	37.1	224.5	13	12.3	13.2	−0.6
well16	Saasaa	Dec-06	W	482	7.4	17.4	12.3	2.3	7	76	31.4	207.4	10.2	31.2	12.2	−0.4
well17	saasaa	Dec-06	W	587	7.1	17.7	15.1	0	10	98	23.7	275.7	13.6	32.6	13.6	3.1

Table 1 continued

Name	Location	Date	Type	EC (μS/cm)	pH (−)	T (°C)	Na^+ (mg/L)	K^+ (mg/L)	Mg^{2+} (mg/L)	Ca^{2+} (mg/L)	Cl^- (mg/L)	HCO_3^- (mg/L)	SO_4^{2-} (mg/L)	NO_3^- (mg/L)	SiO_2 (mg/L)	σ (%)
well18	Saasaa	Dec-06	W	535	7.2	16.4	16.1	3	9	89	21.4	272.1	14.4	29	13.4	1.1
well19	Saasaa	Dec-06	W	557	7.1	17.1	17.2	5.9	10	93	22.2	285.5	16.6	26.4	14	2.4
well21	Saasaa	Dec-06	W	688	7.2	16.5	11.2	2	12	116	103.2	236.7	6	22	13.2	0.3
well22	Saasaa	Dec-06	W	510	7.3	18.2	10.3	1.7	11	87	41.9	225.7	7.9	23.8	12.4	2.8
well23	Saasaa	Dec-06	W	791	7.1	17.5	16	2.4	16	91	95.5	174.5	39.1	30.8	13.6	−1.9
well3	Dorbol	Nov-06	W	560	7.4	14.2	7.4	0	5	107	22.8	274.5	18.2	17.6	14.2	2.3
well2	AboKaook	Dec-06	W	506	7.2	15.7	10.1	3.8	9	93	14.7	256.2	23.5	25.5	11.6	3.6
well3	AboKaook	Dec-06	W	466	7.3	15.6	10.4	2.1	8	85	16	246.4	15	21.1	11.8	2.6
well6	BeitSaber	Nov-06	W	756	6.6	15.6	17.8	1.1	17	121	41.8	246.4	87.2	35.2	10.6	4.3
well2	BeitTima	Nov-06	W	710	6.7	16.7	10.5	1.2	23	121	12.9	224.5	174.6	21.6	14.6	2.7
well3	BeitTima	Nov-06	W	930	6.5	16.7	9.1	1.6	24	167	18.7	285.5	250.7	6.2	10.6	1.2
well1	Hosenieh	Dec-06	W	648	7.2	17	13.5	1.6	15	99	23.7	292.8	52.8	43.6	11.4	−3.5
well2	Hosenieh	Dec-06	W	587	7.3	18.4	10.2	1.2	11	96	19.5	242.8	56.2	32.6	10.6	−0.5
well3	Hosenieh	Dec-06	W	582	7.3	18.7	10.4	1.2	11	90	19.9	240.3	63	24.6	11.4	−2.9
well1	Tabibieh	Nov-06	W	624	7.5	16.3	10.3	1.1	13	104	23.6	240.3	87.3	27.7	9.6	−1.0
well1	Ainashara	Nov-06	W	440	7.3	17.9	8.8	0	10	76	9.3	253.8	5	4.4	27	4.3
well4	BeitSaber	Nov-06	W	588	7.2	14.6	15.2	2.1	13	97	22.4	296.5	15.6	26.4	13.8	3.1
well5	BeitSaber	Nov-06	W	646	7.2	17.3	14.1	1.6	14	102	22.7	251.3	90.4	31.7	11.8	−1.9
well7	BeitSaber	Dec-06	W	473	7.3	15.9	11.5	1.7	7	81	11.8	240.3	17.3	17.6	11.8	2.5
well9	BeitSaber	Dec-06	W	855	7.3	18.8	22.9	0.6	21	140	66.4	198.9	179.8	34.8	19.6	1.7
well1	KaferHour	Nov-06	W	818	7.5	13.3	13	0.8	25	146	14.7	211	314.9	23.8	11	−5.0
well2	KaferHour	Nov-06	W	697	7.5	18.9	11	0	20	116	19.6	240.3	162	19.4	16.4	−1.8
well3	KaferHour	Nov-06	W	673	7.3	19.1	14.8	0.7	17	97	25.1	248.9	78	38.7	17.4	−1.0
well1	Khazrajeh	Dec-06	W	578	7.1	17.2	11	3.1	9	95	22.8	284.3	11.9	26	13.2	0.6
well3	MogherAlMer	Nov-06	W	560	7.4	18	10.4	0	13	85	20.8	297.7	13.9	29.9	12.6	−4.1
well2	Tabibieh	Dec-06	W	662	7.1	17.9	12.6	1.8	15	115	27.9	261.1	89.2	30.8	12	1.0
well1	Talmasiat	Nov-06	W	385	7.4	17	7.1	1.5	7	60	8.7	207.4	6.7	18.9	9.8	−2.2
well2	Talmasiat	Nov-06	W	466	7.4	15.4	6.7	1.3	7	77	8.9	244.1	9.5	23.7	9.2	−0.9
well1	KhanElshekh	Dec-06	W	407	7.4	17.9	9	1	5	73	15.9	203.7	8.3	21.7	10.6	1.9
well2	KhanElshekh	Dec-06	W	625	6.8	17.9	9	1.1	15	128	19.6	274.5	100.6	29.5	11.2	2.9
well4	KhanElshekh	Dec-06	W	443	7.5	19.2	8.6	0.7	5	84	16.1	219.6	16.6	18.9	10.2	3.1
well7	KhanElshekh	Dec-06	W	575	7.1	17.6	11.5	1	13	102	24.8	295.2	26.6	21.6	10.8	2.0
well8	KhanElshekh	Dec-06	W	456	7.4	17.1	11.3	0.8	5	81	19	213.5	17.7	22.9	10.6	2.0
well1	MazratNafor	Dec-06	W	415	7.4	17.7	13.2	1.8	7	62	14.5	214.7	10.1	15.4	11.4	−1.1
well1	Mogher-Hene	Nov-06	W	655	7.2	18.8	16.5	0	15	97	34.9	244	44	44	15.8	1.4

Table 1 continued

Name	Location	Date	Type	EC (μS/cm)	pH (−)	T (°C)	Na^+ (mg/L)	K^+ (mg/L)	Mg^{2+} (mg/L)	Ca^{2+} (mg/L)	Cl^- (mg/L)	HCO_3^- (mg/L)	SO_4^{2-} (mg/L)	NO_3^- (mg/L)	SiO_2 (mg/L)	σ (%)
well2	Mogher-Hene	Nov-06	W	884	7.1	17.2	26.3	0	24	122	61.2	259.9	122.1	81.8	18.6	−3.6
well3	Mogher-Hene	Nov-06	W	541	7.3	18.8	15.3	0.6	10	89	22.5	230.6	35.1	31.7	15.2	2.6
well4	MogherAlmer	Nov-06	W	849	7.2	16.4	27.6	0.7	23	121	53.1	311.1	77	73.5	23	−1.3
well5	MogherAlmer	Nov-06	W	766	7.6	18.1	16.8	0	21	114	38.7	301.1	66	67.8	18.2	−2.2
well6	MogherAlMer	Dec-06	W	529	7.7	19	17.5	0.7	11	75	30.6	173.2	31.2	84	22.4	−2.6
well7	MogherAlMer	Dec-06	W	732	7.3	19.3	22.3	0.8	18	103	61	185.4	35.6	116.6	18.8	1.5
MambejWell	MogherAlmer	Nov-06	W	451	7.2	18.4	6.4	0.8	2	85	9	226.9	7.2	16.3	10.4	3.6
8k	Arneh	Jun-82	W	–	6.9	12.8	9.7	0.7	4.9	22	10.6	91.5	4	6.6	–	0.0
43k	OmSharatet	Oct-84	W	–	7.4	–	6	1.8	18.3	38	21.3	195.2	13	7.1	–	−3.2
46k	AboKaook	Sep-83	W	–	7.1	18	12.2	5	40.2	12	24.8	231.8	2	39.8	–	−1.9
48K	Arneh	Oct-84	W	–	7.4	14	23.9	1.5	18.3	40	14.2	146.4	95	5.3	–	−1.3
49k	Arneh	Oct-83	W	–	7.4	13.5	8.5	0.7	25.6	34	35.5	183	9	5.3	–	−0.2
52K	Beit Tima	Jul-83	W	–	6.5	14.6	29	2	13.4	22	19.5	134.2	32	8	–	−0.3
53K	Beit Tima	Oct-84	W	–	7.5	14.6	8	1.8	12.2	20	17.8	109.8	2	4	–	−0.1
55K	Beit Jinn	May-83	W	–	7.3	11.2	16.6	1.5	9.8	24	14.2	122	23	8.4	–	−0.5
57K	Beit Jinn	May-84	W	–	7.3	10.3	2.5	0.5	14.6	36	12.4	146.4	16	6.6	–	1.6
133K	KhanElshekh	Oct-83	W	–	6.7	20	9.7	9	29.3	20	21.3	207.4	3	2.2	–	−0.3
150k	JdedetArtoz	Aug-83	W	–	7	18	61.6	11	19.5	68	46.1	36.6	300	3.5	–	−1.4
154k	JdedetAartoz	Oct-84	W	–	7.5	–	57.7	4.7	42.7	26	106.5	292.8	9	4	–	−1.9
165k	Dorbol	Apr-85	W	–	8.1	–	2.1	0	19.2	32	21.3	134.2	28	3	–	−1.0
176	JdedetArtoz	Oct-84	W	–	7.5	–	23.5	0.5	17.1	56	49.7	146.4	43	29.6	–	0.1
181	Artouz	Oct-82	W	–	7.3	17.5	29	6.6	18	88	30	260	100	6.6	–	0.1
184K	Beit Saber	Aug-85	W	–	7.4	–	69	12.5	14.4	64	67.4	292.8	45	4.4	–	−0.1
179	Artouz	Oct-82	W	–	8.2	18	17	2.5	24.3	52	30	165	80	8	–	0.5
186	KhanElshekh	Apr-83	W	–	6.2	–	62.1	1.3	19.5	60	35.5	237.9	104	14.1	–	0.3
265k	KaferQuaq	Dec-84	W	–	7.3	18	2.3	3.1	32.2	64	65.1	179.8	72	9.3	–	−3.3
275k	Arneh	Oct-85	W	–	7.5	–	18.4	4.3	31.2	124	49.7	317.3	150	0	–	−0.1
300	KhanElshekh	Oct-84	W	–	7.6	16.5	37.5	2.3	19.5	52	28.4	244	42	8.4	–	0.1
720	KhanElshekh	Mar-85	W	–	7.3	20	0.9	0	43.2	36	35.5	231.9	5	26.5	–	0.3
721	Qatana	Apr-85	W	–	7.7	19	48	21.5	2.4	64	28.4	170.8	70	61.9	–	0.6
721a	Qatana	Apr-85	W	–	7.4	–	11.5	2.3	7.2	64	35.5	183	15	8.8	–	−0.7
740	KhanElshekh	Aug-85	W	–	7.4	20	16.1	2.3	16.8	56	60.35	183.1	4	8.3	–	0.0
744	KhanElshekh	Aug-85	W	–	7.4	–	31.8	3.1	21.6	44	35.5	239	15	11.1	–	0.5
3032	Kafer Qouq	May-84	W	–	8.2	–	27.6	0.5	12.2	52	21.3	213.5	17	8	–	2.3
3036	Qatana	Oct-84	W	–	7.3	17	53.8	3.2	3.7	86	56.8	274.5	18	31.8	–	0.1

Table 1 continued

Name	Location	Date	Type	EC (μS/cm)	pH (−)	T (°C)	Na^+ (mg/L)	K^+ (mg/L)	Mg^{2+} (mg/L)	Ca^{2+} (mg/L)	Cl^- (mg/L)	HCO_3^- (mg/L)	SO_4^{2-} (mg/L)	NO_3^- (mg/L)	SiO_2 (mg/L)	σ (%)
3050	Saasaa	Jun-82	W	–	8.4	17.4	35	1.8	35	11.6	70	128	18	13	–	3.9
3055	Kleaa	May-84	W	–	8.2	–	12.2	1.5	9.8	28	10.7	128.1	10	5.3	–	1.9
3072	Heneh	May-84	W	–	7.5	14.4	61.9	0.3	25.6	58	49.7	176.9	145	23.4	–	0.2
BeitJinn	BeitJinn	Nov-06	S	284	8.1	12.3	3.6	1.3	8.5	47	14.9	156.2	8.7	2.6	5.4	0.5
Almalha	Arneh	Nov-06	S	972	7.1	13.4	5.1	0.8	29	183	4.2	234	395	2.6	5.6	−2.3
Arneh	Arneh	Nov-06	S	261	8	11.5	2.9	0.4	3.5	53	5.1	168	3.7	1.8	4.4	1.1
Albardeh	Arneh	Nov-06	S	640	7.4	13.7	5	1.2	15	120	6.5	248	164.5	5.3	6.2	−2.1
Almshraa	Arneh	Nov-06	S	470	7.6	10.7	3.1	0	15	74	4.1	144	116	1.3	4.2	1.6
Dorbol1	Dorbol	Nov-06	S	295	7.8	17.6	3.6	0	2.5	54	7	164.7	7.6	2.9	6.6	−0.7
Dorbol4	Dorbol	Nov-06	S	251	7.9	14.5	2.8	0	4	42	6.4	139	3.7	4	4.8	−1.1
Dorbol3	Dorbol	Nov-06	S	245	7.7	15.2	2.8	0	3	40	5.6	136.6	4.3	3.8	5.4	−3.8
RasAlin	Qatana	Nov-06	S	330	7.4	17.6	5.8	0.7	8	58	7.8	185	6.1	10.1	6.6	3.9
Hamana	BeitTima	Nov-06	S	789	7.1	17.6	12.4	1.7	25.5	133	25.6	289.1	168	15.4	22	0.7
Beitsaber1	Beitsaber	Nov-06	S	762	7.1	17.2	10.2	0.8	23.5	131	20.2	290.4	132	11.9	12.4	4.2
Beitsaber2	Beitsaber	Nov-06	S	767	7.1	16.7	11.6	0.9	23	132	18.8	307.4	136	20.2	12.6	1.7
Alla	Ainashara	Nov-06	S	327	8.1	16.1	8.3	2.2	2.5	52	13.5	109.8	14.9	27.7	6.8	4.7
KaferHour1	KaferHour	Nov-06	S	887	7.3	15.8	13.6	6.6	25.5	153	35.5	327	171	29.9	13.8	0.5
Talmasiat	MogherAlMer	Nov-06	S	345	7.4	15.9	13.1	3.4	6	53	10.2	195	7.2	9.7	16	−0.6
Ganat	Hasebe	Dec-06	S	462	7.4	18.1	7.6	2	8	74	12.9	224.5	36.3	18	9.2	−3.8
AinAljoz	Kalaetjandal	Nov-06	S	219	7.8	14	2.9	0.5	9.5	30	3.8	137	2.9	1.9	5	−0.5
jandal	KalaetJandal	Nov-06	S	403	8	16.2	12.7	2.5	16.5	45	23.8	103.7	23.5	80.5	7.2	0.7
Mambej	MogherAlmer	Nov-06	S	325	7.7	16	13.9	3.7	6	51	6.6	190	5.7	8.8	15.2	2.5
Bkassam1	Bkassam	Nov-06	S	670	7.9	15.5	29.5	4	26	61	57.1	156.2	35.2	122.8	7.8	−2.4
BeitJinnn Ala	BeitJinnn	Nov-06	S	260	8.4	11.2	1.8	0.5	7	42	2.1	136.6	13	1.7	3.6	3.2
Morkos	Arneh	Dec-06	S	610	7.6	12.4	2.1	0	14	107	4.1	153.7	196.2	2.6	5	−1.5
Kneseh	Remeh	Dec-06	S	428	7.6	13.4	5.7	1.6	8	74	8.6	229.4	18.6	15.4	7.6	0.0
Tamer	Remeh	Dec-06	S	315	7.7	14.1	4	0	9	46	6.7	173.2	9	9.2	7	−2.4
Dorbol2	Dorbol	Nov-06	S	298	7.3	16.8	3.5	0	2	57	6.6	172	5.2	4	5.8	−0.3
Saasaa	Saasaa	Nov-06	S	237	7	18.4	19.7	4.5	8.5	15	13.1	80.5	8.9	19.8	27.6	5.0
Bkassam3	Bkassam	Nov-06	S	535	7.7	12.1	5.1	0	21	75	6.4	180.6	95.8	28.1	6.6	1.0
AinBala	Qatana	Nov-06	S	582	7.4	17.4	10.5	0.7	8	115	12.2	266	67	12.3	12	4.6
Bkassam2	Bkassam	Nov-06	S	633	8.1	16.4	22	5.9	20	76	39.2	201.3	25.2	104.3	8.6	−0.5
Asfal	Ainshara	Nov-06	S	318	7.5	15.4	4.7	1.3	3	63	7	178.1	6.3	5.3	6.4	4.3
KhrbtSouda	KhrbtSouda	Nov-06	S	262	8.1	13.4	3.5	0	1	41	6.3	127	8.5	3.1	5.4	−4.4
33	Tal Assyuf	Jun-83	S	–	7.5	–	142.9	0	41.5	108	140	280.6	59	4.2	–	1.1

Table 1 continued

Name	Location	Date	Type	EC (μS/cm)	pH (−)	T (°C)	Na^+ (mg/L)	K^+ (mg/L)	Mg^{2+} (mg/L)	Ca^{2+} (mg/L)	Cl^- (mg/L)	HCO_3^- (mg/L)	SO_4^{2-} (mg/L)	NO_3^- (mg/L)	SiO_2 (mg/L)	σ (%)
41	Ain Saba	Dec-77	S	–	7.5	–	10	0	23	85	14	207.4	134.1	0	–	0.8
43	Rashasheh	Sep-77	S	–	7.2	–	13	0	26	89	17.4	231.8	135	0	–	0.4
44	Rijmeh	May-83	S	–	8.1	–	9.2	0	18.3	18	12.4	134.2	7	0	–	2.0
45	Ras Alwadi	Jul-78	S	–	7	–	20	0	12	38	25	170.8	10.7	0	–	0.4
46	Tabibieh	Aug-82	S	–	8.2	–	14.7	0	7.2	52	10	150	42	13.2	–	0.0
47	Husenieh	Oct-83	S	–	6.9	–	15.6	0	3.6	32	19.5	109.8	6	3.1	–	1.0
49	Mbaya	Oct-83	S	–	7.6	–	13.3	0	7.3	24	17.8	109.8	2	2.2	–	0.0
51	Artouz Qanat	Aug-84	S	–	7.5	–	26.4	0	4.9	60	46.2	145.2	18	26.4	–	0.7
61	Alfouar spring	Oct-83	S	–	6.9	–	11.7	0	4.9	12	17.8	48.8	2.5	2.7	–	3.9
10276	Mt Hermon	Oct-84	S	–	7.3	–	21.6	2	20.7	42	21.3	183	50	10	–	−0.1
10285	Shabaanet	Oct-84	S	–	7.6	–	73.6	0.5	25.6	66	21.3	256.2	180	5.4	–	−0.1
10291	Mt Hermon	Oct-84	S	–	7.7	–	1.4	0.4	25.5	60	99.4	128.14	4	8.4	–	0.5
10292	Ain Najeem	Oct-84	S	–	7.8	–	4.6	0	19.3	116	61.4	97.6	190	8.8	–	1.3
10297	Almashraa	Oct-84	S	–	8.3	–	23	0	24.3	50	76.5	122	33.4	11.3	–	4.6
10308	Beit Tima1	Oct-84	S	–	7	–	6.7	0.4	34.8	72	31.3	176.9	130	18.1	–	0.2
10309	Beit Tima2	Oct-84	S	–	7.1	–	4.6	3.5	60	104	139.5	30.5	283.4	4.4	–	0.6
10310	Mt Hermon	Oct-84	S	–	7.7	–	0	0	24.3	22	17.8	122	20	2.6	–	2.1
10311	Mt Hermon	Oct-84	S	–	7.3	–	4.6	3.5	18.2	52	32.3	91.5	88.9	8.8	–	−0.3
10322	Mt Hermon	Dec-84	S	–	7.7	–	2.7	0	24.3	84	83.4	122	76.8	21.6	–	0.1
10325	Mt Hermon	Dec-84	S	–	7.7	–	0.5	0	14.6	32	30.9	74.4	31.2	6.2	–	−0.3
10326	Mt Hermon	Dec-84	S	–	8.1	–	0.2	0	12.2	20	21.3	62	10	5.7	–	2.3
10327	Albardeh(Remeh)	Dec-84	S	–	8.3	–	2.3	0.8	23.1	64	81.7	115.9	38.9	21	–	−1.3
10333	Ain Badran	Dec-84	S	–	7.9	–	0.3	0.8	24.3	36	35.5	122	29.7	8	–	1.2

EC electrical conductivity, *W* well, *S* spring, *σ* chemical analyses error

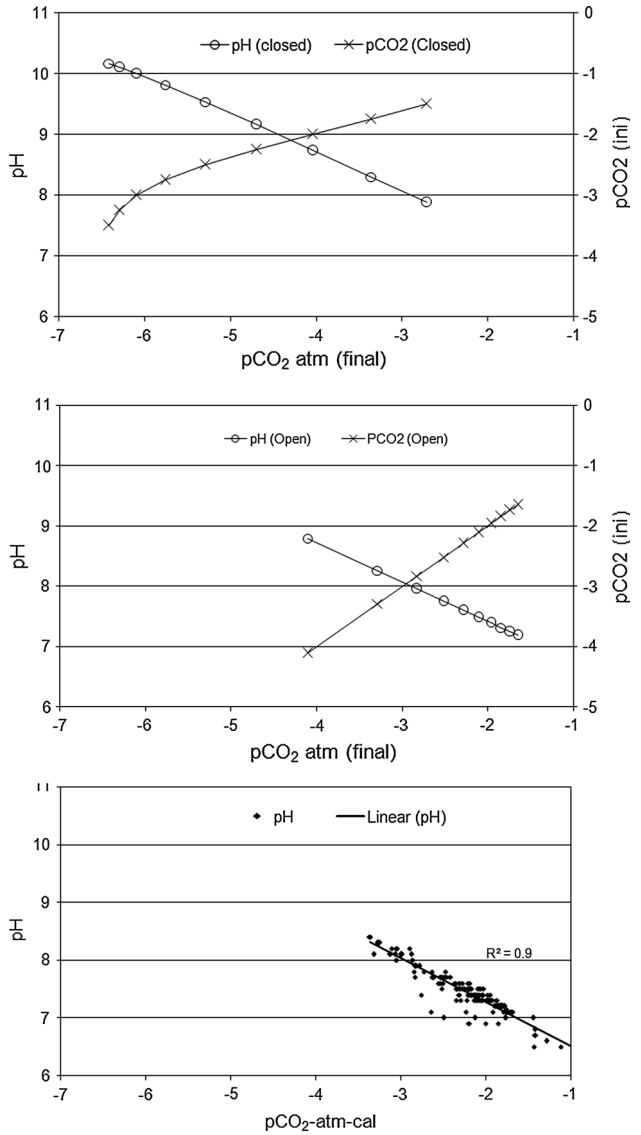

Fig. 3 Open and closed system dissolution of carbonate system determined with PHREEQC and pH values as a function of pCO_2 (atm) calculated values in the water samples

The scatter plot of saturation indices (SI) of calcite and dolomite is shown in Fig. 4b. In this diagram, a central band of 0.4 units wide along each axis, representing errors that may occur in the measurement of pH, Mg^{2+}, and Ca^{2+}. The four quadrants of the plotting field (I–IV) represent different kinds of equilibrium conditions with respect to calcite and dolomite. The figure shows that some of the water samples are distributed in quadrant I and III, and most of them are situated in the central band of equilibrium. The samples in quadrant I represent supersaturation with respect to both carbonates. The samples plotting in quadrant III represent undersaturation with respect to calcite and dolomite. These samples correspond to water coming from an environment where carbonates are impoverished, or to water that has a short residence time in the hosting carbonate rocks (Langmuir 1971; Kortatsi 2007).

The SI of calcite as a function of calculated pCO_2 are shown in Fig. 5 (chart), and are mainly closed to or exceed zero for most samples and the spatial distribution of SI of calcite is shown in Fig. 5 (map). The highest part of the Jurassic is characterized by low SI of calcite, whereas relatively high values were measured in the lower part levels near the Arneh village. This is mostly due to a short residence time and a lesser amount of CO_2 as a result of vegetation absence in the higher parts characterized by limited soil development. The low SI of calcite near the Arneh village might indicate a quick groundwater circulation from the north part towards the south part through channels and conduits developed along faults and fractures as a preferential flow. The high values encountered in the alluvial and basalt aquifers can indicate a deep groundwater flow from Jurassic aquifers to these aquifers controlled by sub-regional geological structures.

The alternation of limestone and dolomite along the flow path can be characterized by Mg/Ca ratios. Mg/Ca ratios between 0.5 and 0.9 are typical for carbonate aquifers (Hsu 1963; Stadler et al. 2012). For groundwater genetically bound to pure limestones, the Mg/Ca ratio is smaller than 0.1 on the other hand, water from pure dolomite is characterized by Mg/Ca ratios higher than 0.7 (Flakova 1998). However, even very pure limestone can give rise to relatively high Mg/Ca ratios in water with a long residence time (Moral et al. 2008; McMahon et al. 2004; Batiot et al. 2003; López-Chicano et al. 2001; Edmunds and Smedley 2000; Fairchild et al. 2000; Plummer et al. 1978; Plummer 1977; Bicalho et al. 2012). In fresh water, Mg/Ca ratio values greater than 1 can be the result of water interacting with Mg-rich silicate rocks such as volcanic ones, with Mg being derived from olivine (Schoeller 1956; Hem 1985; Vengosh and Rosenthal 1994).

Figure 5 (chart) shows that most of the samples indicate Mg/Ca ratios less than one and many of them less than 0.5. These values imply that the contact time between the infiltration water and hosting rocks was rather short. Few samples show ratios superior to 1 indicating a basaltic rock weathering or precipitation of gypsum resulting from an impoverishment in Ca ions, or sulphate reduction process facilitated by anaerobic conditions.

The dissolution of gypsum leads to increasing sulphate concentration in groundwater and to enhanced solubility of dolomite; consequently it lowers the solubility of calcite. SI of gypsum as a function of SO_4^{2-} concentration are plotted in Fig. 6. The relationship between the two variables shows that the dissolution of gypsum is the main source of sulphate in these waters (correlation coefficient $r = 0.64$). This is associated with an increase in calcium

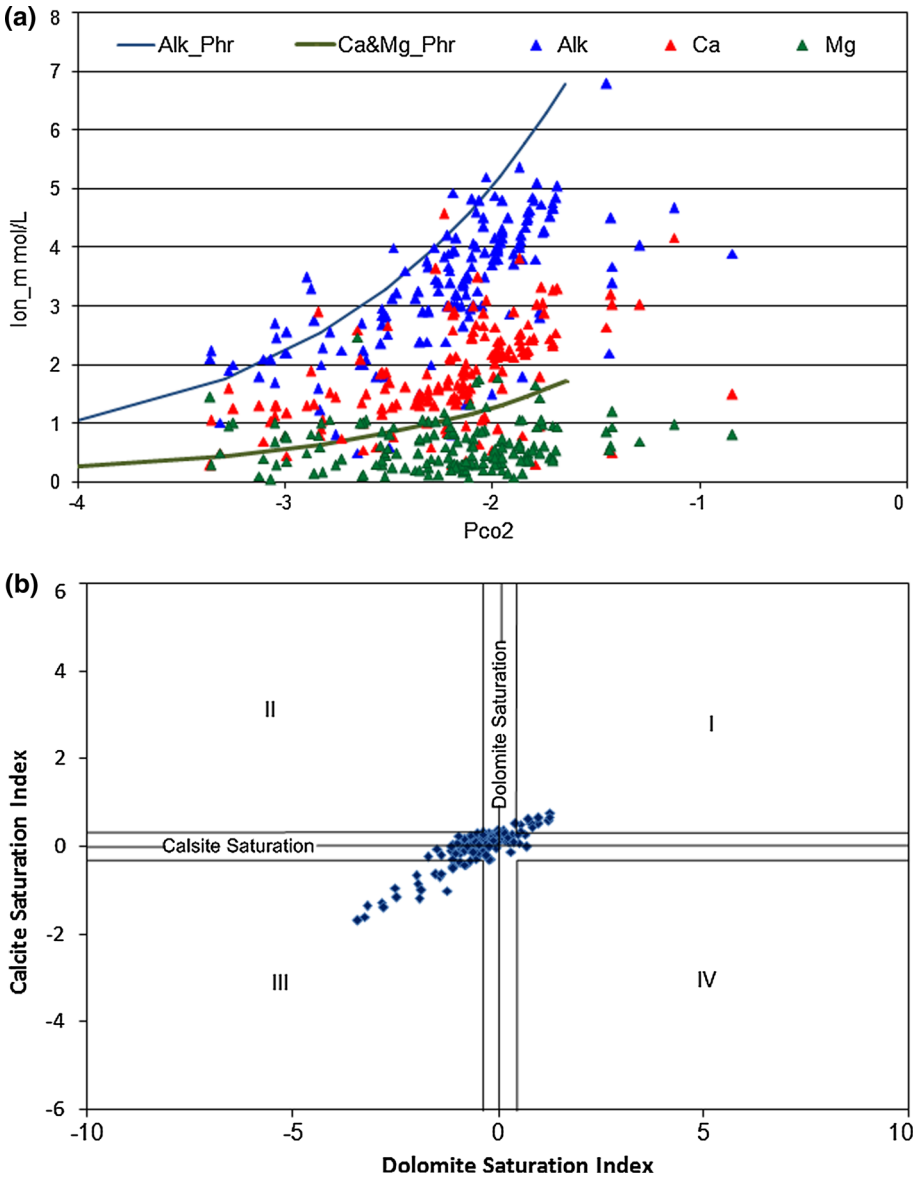

Fig. 4 **a** Calcium, magnesium, and alkalinity concentration in mmol/L as a function of pCO_2 (atm) calculated values; *solid lines* are the alkalinity, calcium, and magnesium determined with PHREEQC for pure calcite and dolomite dissolution. **b** The saturation indices (SI) of calcite and dolomite determined in the water samples

concentration as shown in Fig. 7. This figure shows also that there is no correlation between calcium and sulphate for all the samples only when sulphate concentration becomes greater than 0.5 mmol/L. The trend indicates a positive relationship between the two variables due to gypsum dissolution.

Dedolomitization process

The occurrence of Mesozoic limestones and dolomites associated with gypsiferous layers gives rise to Ca-sulphate-rich water which induces dissolution–precipitation processes in the dolomite–calcite mineral assemblage (Capaccioni et al. 2001). Dedolomitization process means, that the calcite precipitation and dolomite dissolution are driven by anhydrite (gypsum) dissolution (Plummer et al. 1990). The dedolomitization is controlled by the three following reactions:

$$CaSO_4 \rightarrow Ca^{2+} + SO_4{}^2 \quad (1)$$

$$Ca^{2+} + 2HCO_3{}^- \rightarrow CaCO_3 + CO_2 + H_2O \quad (2)$$

$$2CO_2 + 2H_2O + CaMg(CO_3)_2 \leftrightarrow Ca^{2+} + Mg^{2+} + 4HCO_3{}^- \quad (3)$$

The increasing concentration of Ca^{2+} during the dissolution of gypsum leads to the precipitation of calcite. A decrease in $HCO_3{}^-$ concentration causes the dissolution of dolomite and an increase in Mg^{2+} concentrations in water. The increasing in Mg^{2+} concentrations causes an increase in Ca^{2+} concentration, until the equilibrium is reached between water and both minerals. Thus, the gypsum dissolution brings about a substitution of dolomite by calcite.

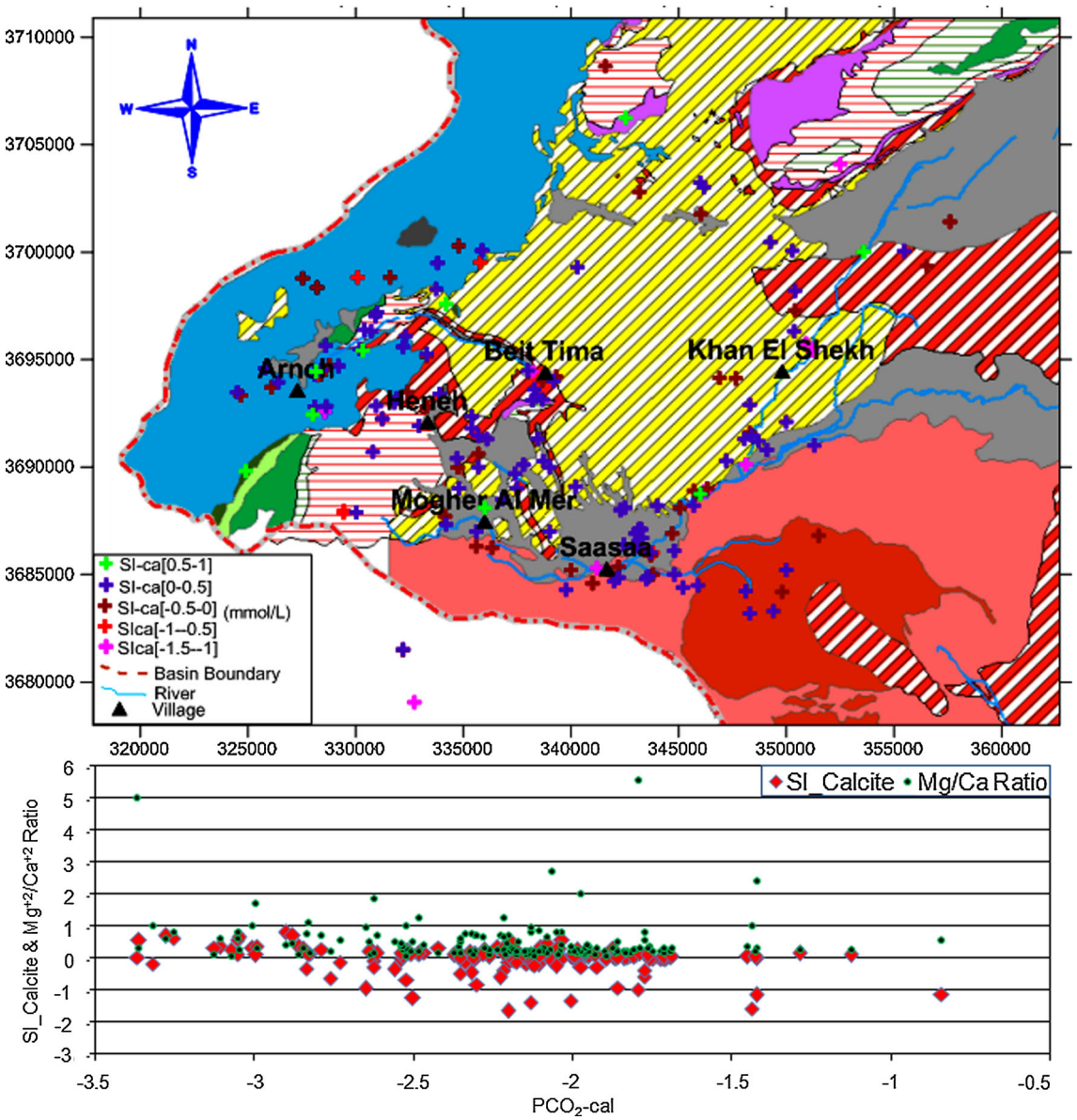

Fig. 5 Classification and spatial distribution of saturation index of calcite in the water samples with chart showing the SI of calcite and Mg^{2+}/Ca^{2+} molar ratio as a function of pCO_2 (atm) calculated values

In the thermodynamic calculation, it is likely that gypsum dissolution is irreversible in most of the system, whereas the water remains at or near saturation with respect to calcite and dolomite. It is appropriate then to choose the dissolved sulphate as a reaction progress variable in examining the trend in the water quality data (Plummer et al. 1990) (Fig. 6). The samples that are characterized by low saturation indices of calcite and by low concentration in sulphate (<1 mmol/L), indicate that little or no gypsum dissolution occurred for these water samples. Some samples show over saturation of dolomite even with less content in sulphate, indicated that the dolomite dissolution was not driven by gypsum dissolution. When the sulphate concentration increases for some samples, they become near saturation with respect to dolomite if we accept an uncertainty of about ±0.5 for saturation index determination. The majority of these samples are located in the Jurassic aquifer. SI of gypsum as a function of sulphate concentration evolve from undersaturated to quasi-saturated and sulphate concentration increases with the development of gypsum dissolution. Figure 7 shows that the high values of sulphate (more than 1 mmol/L) which are associated with over saturation with respect to dolomite were measured mainly near the Arneh village. It indicates that the dedolomitization process is occurring there. This phenomenon was observed near Beit Tima and south of

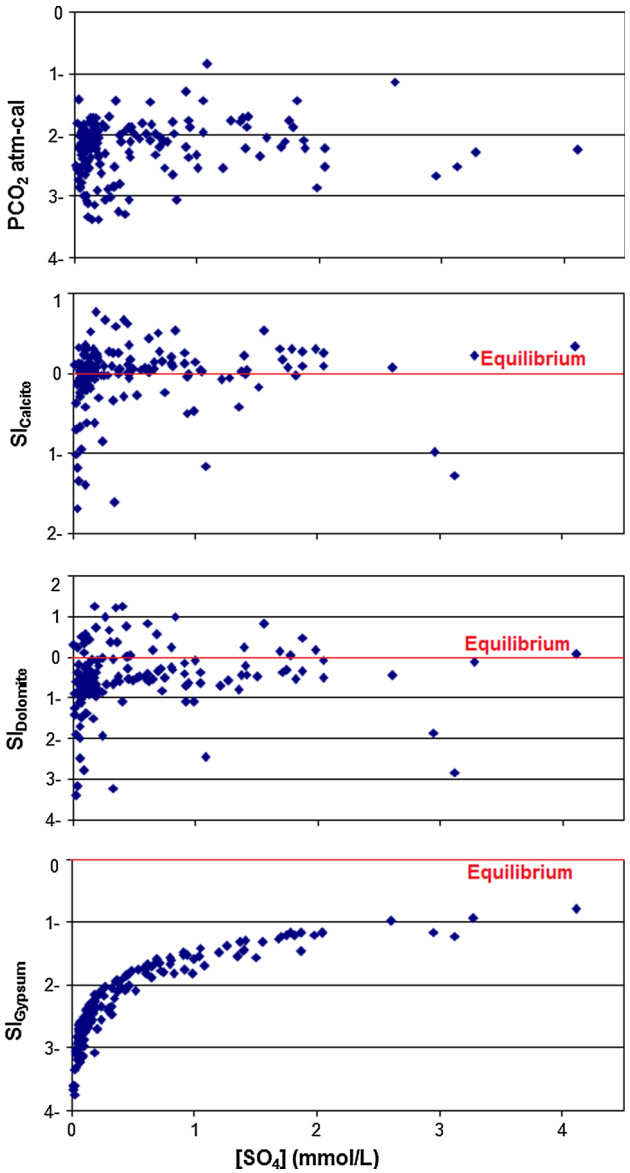

Fig. 6 Saturation indices of calcite, dolomite, and gypsum as well as pCO_2 (atm) calculated values as a function of SO_4^{2-} (mmol/L)

Heneh villages (Miocene aquifer). Other high concentrations of sulphate which are not associated with over saturation of dolomite indicate additional sources of sulphate such as anthropogenic influences. As a consequence of dedolomitization reactions, the calcite precipitation in the system causes a decrease of pH values due to H^+ released from HCO_3^- during the incorporation of CO_3 to calcite. In our case, the pH values are hardly going down as shown in Fig. 7. According to Figs. 6 and 7, we can conclude that an approach to dedolomitization processes only occurs in isolated places where the gypsiferous formations are located.

Silicate weathering

The effect of silicate weathering on the water chemistry is primarily the addition of cations and silica, given that high silica in the water samples indicates active hydrolysis of silicate minerals.

The silica values for the samples collected in 2006 are shown in Fig. 8. Clearly, a sharp boundary between three groups is observed. The first one is characterized by low silica concentrations and located in the Jurassic aquifers. The second one is located in the Neogene and Quaternary formations and characterized by higher silica. The highest concentration in silica, (third group), was observed in the basaltic Miocene aquifer which is more weathered compared to the basalt of the Quaternary. High silica content In the Neogene/Quaternary aquifers might indicate a flow pattern from the Miocene basaltic aquifer to the southeast direction toward these aquifers.

The mineral stability diagram is another approach to test the proposed hydrochemical evolution (Drever 1988; Guler and Thyne 2004b). The stability fields for the Na-Plagioclase (albite) and its potential weathering products, paragonite, gibbsite, kaolinite, and pyrophyllite are shown as a function of log ($[Na^+]/[H^+]$) and log $[H_4SiO_4]$ in Fig. 8. It shows that the main reaction is the conversion of albite to kaolinite. Meaning that the primary silicate minerals, such as plagioclase and clinopyroxene, can be dissolved and weathered to kaolinite which is most likely to be in equilibrium with groundwater. While noting some samples extending into the albite stability field suggesting equilibrium between clay and primary mineral, it is not likely to be the main process controlling the water chemistry.

Figure 8 also shows the stability fields for the Ca-Plagioclase (anorthite) and its possible weathering products, gibbsite, kaolinite, and Ca-montmorillonite as a function of log ($[Ca^{2+}]/[H^+]^2$) and log $[H_4SiO_4]$. In this case, the kaolinite is more likely to be stable than for example gibbsite, as a result of anorthite weathering products. This may be due to removal of the Ca from the system by the precipitation of Ca salts. Some samples which are located at or close to the stability field of montmorillonite indicated that the typical aquifer of these water samples is basically a basic rock (like basalts) (Appelo and Postma 2005).

The two diagrams show that most of the groundwater samples are not in equilibrium neither with albite nor with anorthite, and they will decompose if they are present in the system.

According to Han and Liu (2004), we can use the variation in the composition of water (Mg^{2+}/Ca^{2+} and Na^+/Ca^{2+}) to distinguish limestone, dolomite, and silicate rock sources of ions. Figure 9a displays the covariation between the two molars ratios. These two ratios are

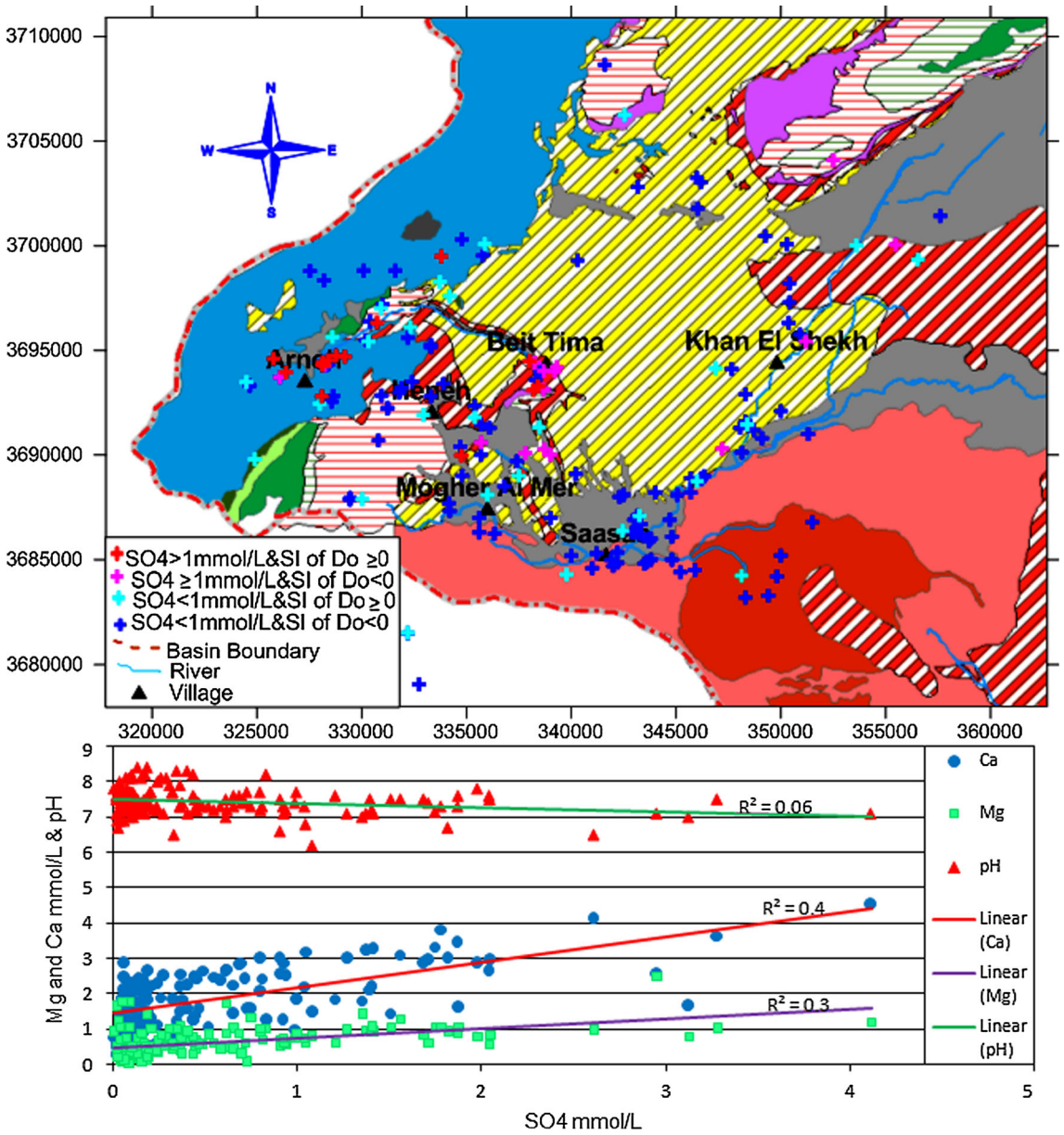

Fig. 7 Classification and spatial distribution of saturation index of dolomite in the water samples, and a scatter charts of Ca^{2+}, Mg^{2+} (mmol/L) and pH as a function of SO_4^{2-} (mmol/L)

almost equivalent because both of them vary over three orders of magnitude. Water samples composition seems to be affected by the mixing trend of three types of rock, most likely the carbonate rocks have a higher effect. It is noticeable that the Mg^{2+}/Ca^{2+} ratios of most samples are bellowing the $Mg^{2+}/Ca^{2+} = 0.8$ line. This is probably due to equilibration of the water simultaneously with calcite and dolomite. The water equilibrated together with calcite and dolomite gives an ideal molar Mg^{2+}/Ca^{2+} ratio of about 0.8 (Appelo and Postma 1993; Han and Liu 2004).

Dissolved solutes and nitrate concentrations

The intensive uses of fertilizers and manure in the agricultural management systems have increased the nitrate pollution of groundwater and have adverse effects on ecosystems and human health (Anastasiadis 2003). Biodegradation of crop residues, agricultural and municipal wastes applied to agricultural fields and waste generated directly by animals are also considered as other sources of nitrate pollution. Figure 10 shows that the low nitrate concentration was mostly measured in

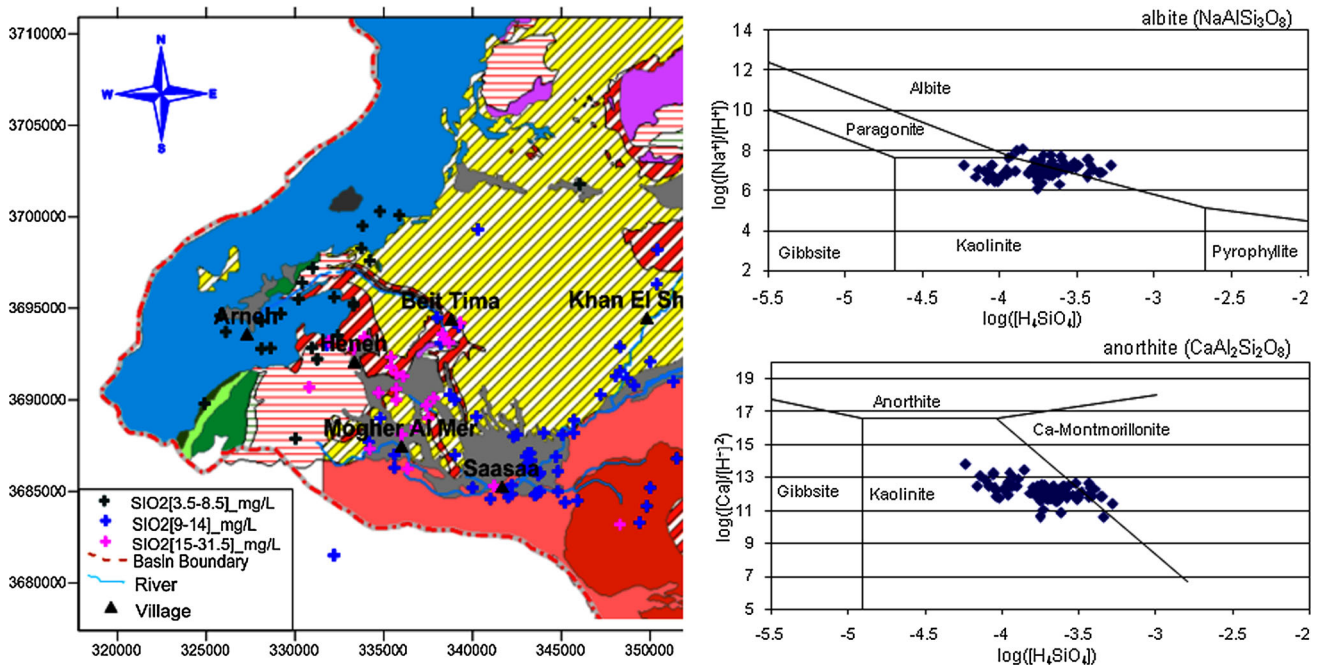

Fig. 8 Classification and spatial distribution of SiO_2 (mg/l) concentration in water samples and stability diagram of both Ca-Plagioclase (anorthite) and Na-Plagioclase (albite) and their possible weathering products

the mountain area (Jurassic and Paleogene aquifers) where there are less agricultural activities. On the other hand, this parameter tends to increase in the plain area (Neogene and Quaternary aquifers). These two aquifers host a considerable number of irrigation wells and intensive agricultural activities using massive input of nitrogenous fertilizers and manures. The effect of irrigated return flow on the groundwater seems to be significant in this area. Inorganic agricultural fertilizers are also thought to be the major sources of chloride in the groundwater. Few water samples are characterized by considerable chloride concentrations associated with relatively high nitrate concentrations as shown in Fig. 10. The high chloride concentration might be attributed to geochemical processes associated with evaporite dissolution. The upward leakage from deeper aquifers, where these formations are located, increases the chloride concentration.

Redox processes

Based on the relationship between pH and Pe, Fig. 9b shows the stability diagram of redox conditions range within the aquifers. It can be stated that the redox conditions in the aquifers vary from aerobics to suboxic conditions, because no redox couple is clearly present in this case.

Stuyfzand classification

In hydrochemical studies, classification serves the purpose of isolating a group of representative clusters (also known as water groups or hydrochemical facies). This can be correlated with location and geology (Suk and Lee 1999; Barbieri et al. 2001; Guler et al. 2002; Guler and Thyne 2004a).

The predominant water types are determined and schemed (Fig. 11) using the Stuyfzand method (Stuyfzand 1989). According to this method, groundwater can be classify as very oligohaline, oligohaline and fresh (Cl^- <150 mg/L for all sample except one then the code changes between G, g and F). The factor F is mainly dominant in the southern and southeastern parts of the area (plain part) as a result of intensive irrigation activities associated with high evaporation rates and return flow as well as the effect of topographic factor. The upward leakage from deeper aquifers, where evaporites are present, can be another source of chloride. In terms of alkalinity values, the groundwater is classified as moderately low, moderate and moderately high (alkalinity varying between 1 and 8 meq/L then the code changes between 1, 2, and 3). HCO_3^- concentration increases with the general direction of the flow pattern. This indicates the effects of carbonate rocks dissolution by infiltrating CO_2-rich meteoric water and dissolution of volcanic rocks. The local appearance of

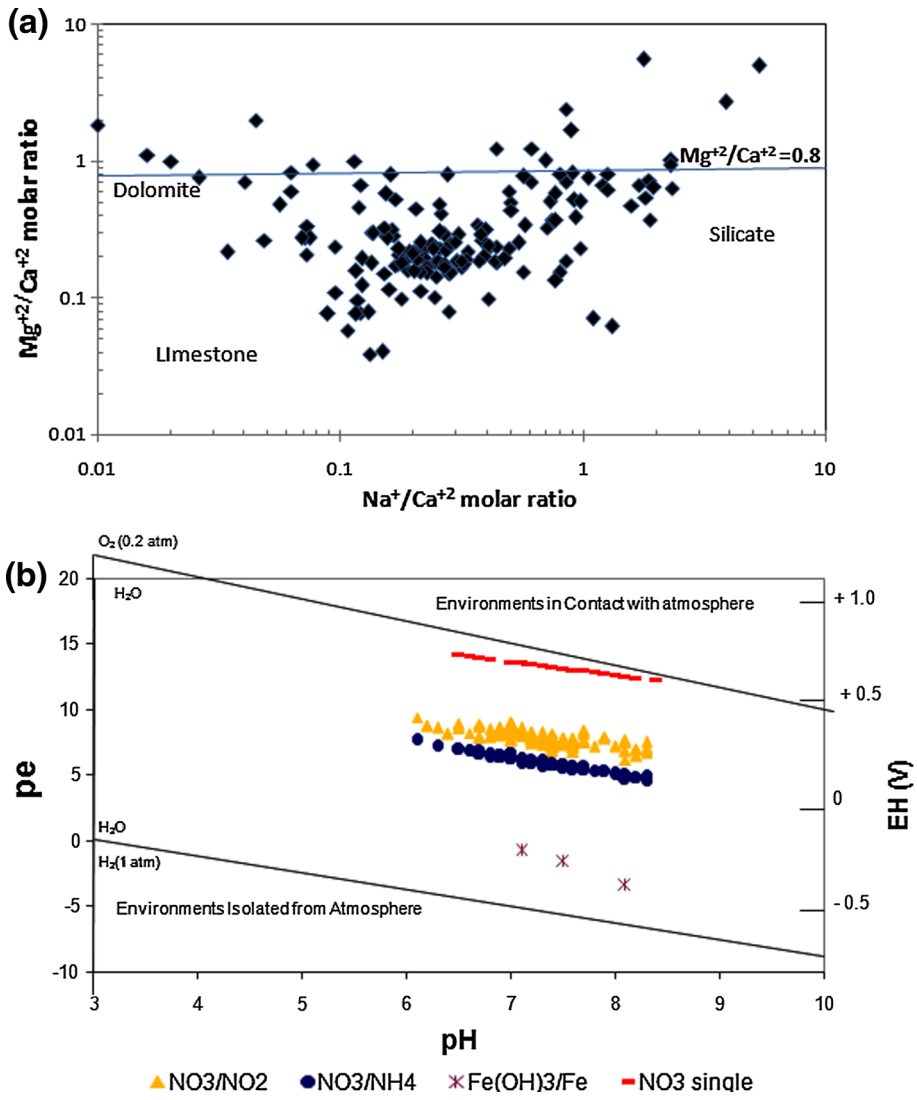

Fig. 9 **a** Na^{+}/Ca^{2+} versus Mg^{2+}/Ca^{2+} molar ratios in the water samples, (after Han and Liu 2004). **b** The stability diagram of redox conditions range based on the relationship between pH and Pe and the distribution of water samples

Ca-NO_3 water types in the plain area is a result of agricultural pollution. In the western part, mainly in the Jurassic aquifer, the calcium mix water type is present. The "Mix" anions water type refers to all the water in which no anion family makes up more than 50 % of the sum of anions. Generally, the HCO_3^- is the dominating anion and Ca^{2+} is the dominating cation of the hydrochemical types of groundwater in the whole area.

Groundwater flow behaviour

According to water type classification, groundwater discharge (mainly major springs), and geological and structural control, the study area can be divided into four subareas S_1, S_2, S_3, and S_4 (Fig. 12).

The groundwater flows in S_1 from the north and northwest in Mt. Hermon towards the south and southeast through the karstic channels and conduits. Groundwater in R1 discharges in many springs located in the valley around the Arneh village; together these springs form one of the two tributaries of the Awaj River (Sebarani). In S_2, groundwater also flows in karstic channels in the Jurassic aquifer towards the south and east direction afterward discharging in the Upper Beit Jinn spring. In this area, another tributary of the Awaj River (Jinani) is generated. The average annual discharge of upper Beit Jinn spring is very close to the volume of the annual rainfall amount estimated over S_2 (RDAWSA 2006), and since the infiltration coefficient is estimated to 84 % for this area (RDAWSA 2006), the recharge area might not correlate with the size of the geographic surface water catchment. Therefore, the basin boundaries can be extended towards the west (Fig. 12). In S_3, groundwater flows towards Beit Jinn spring and it is also controlled by faulting and structural blocks. S_4 is the biggest subarea which includes the

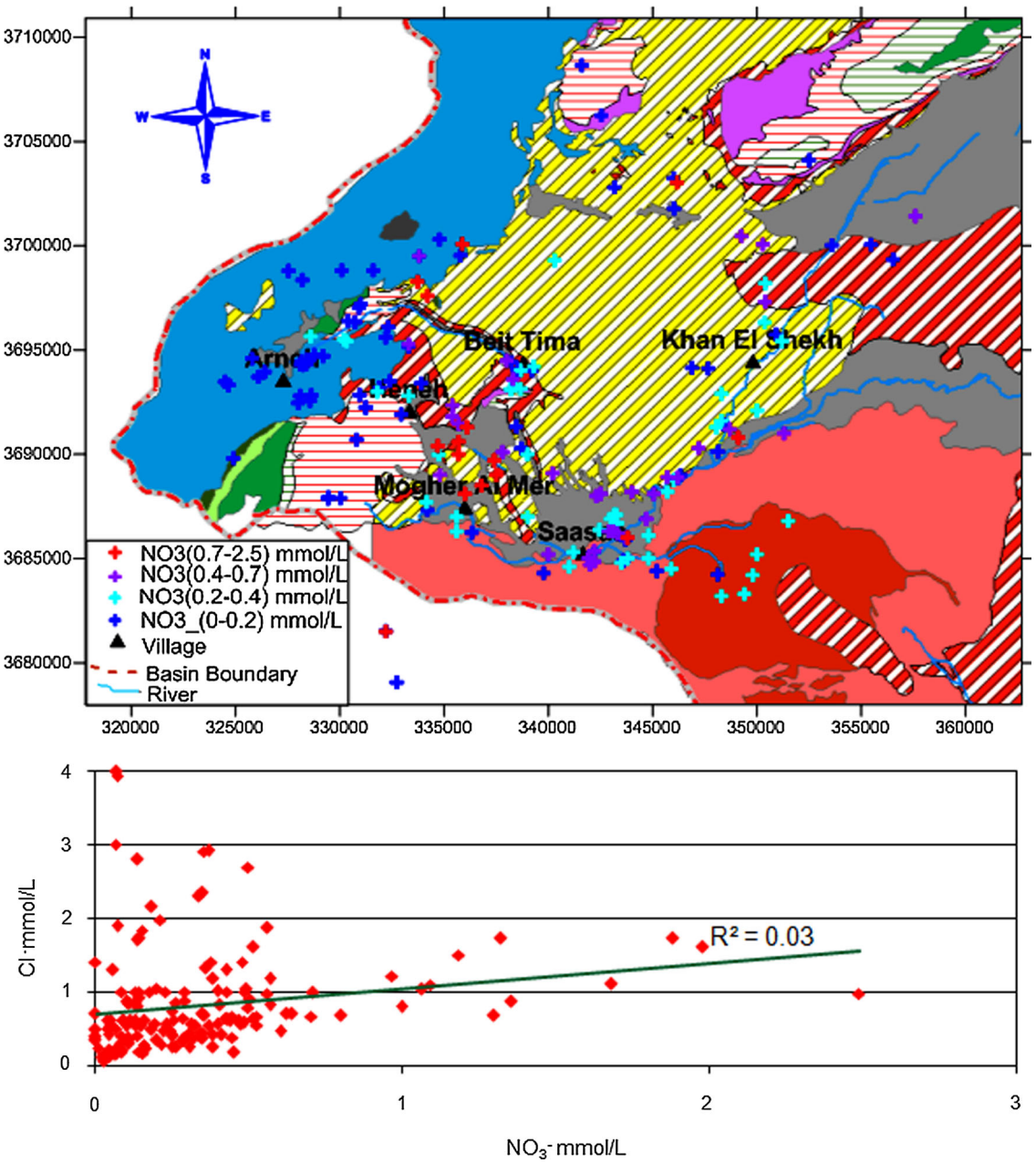

Fig. 10 Classification and spatial distribution of NO_3^- concentrations (mmol/L) and its relationship with Cl^- concentration (mmol/L)

zones with higher groundwater withdrawals for intensive irrigation purposes. The Neogene and Jurassic outcropping formations are the main sources of the water recharge in S_4 but it also receives the input of the upper Paleogene, Quaternary and Miocene basalt aquifers. In this area, water discharges through the major springs, Membeg, Talmassiat, Tell assyouf, and Tabibieh located from west to east. Numerous wells also exist in the Neogene conglomerate aquifer which is recharged from both the direct infiltration and the hydraulic exchange with the deeper Jurassic and Cretaceous aquifers. At the level of a major northwest-southeast fault cutting through the Neogene Plain, water is thought to converge to Tabibieh Spring. This spring originates in the east–west fault along the Awaj River.

Conclusion

The use of hydrochemistry in this case study has provided useful information about the different mechanisms

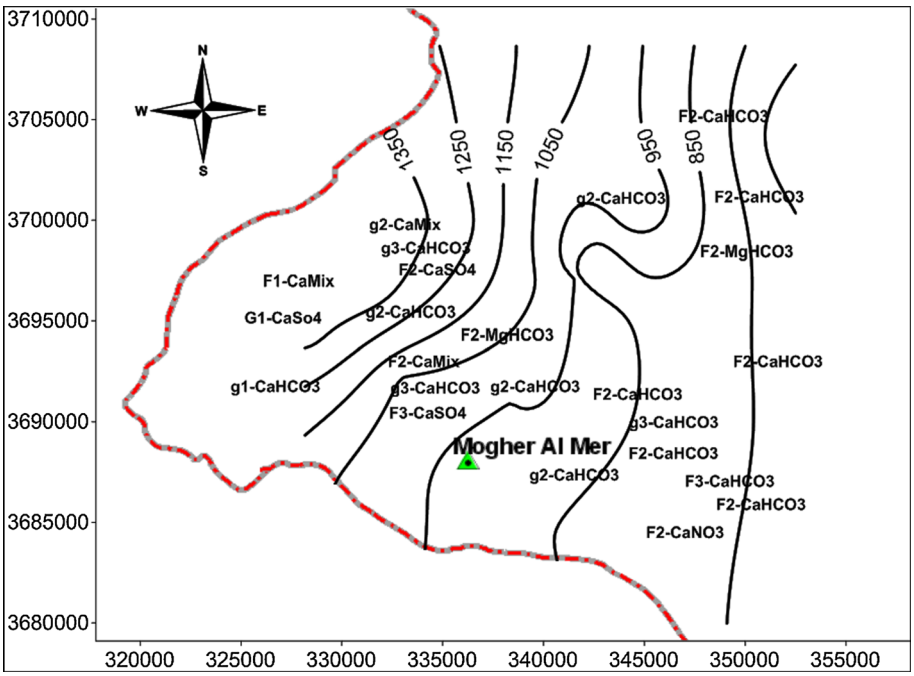

Fig. 11 Equipotential contour map for December 2006 and associated water type based on Stuyfzand classification

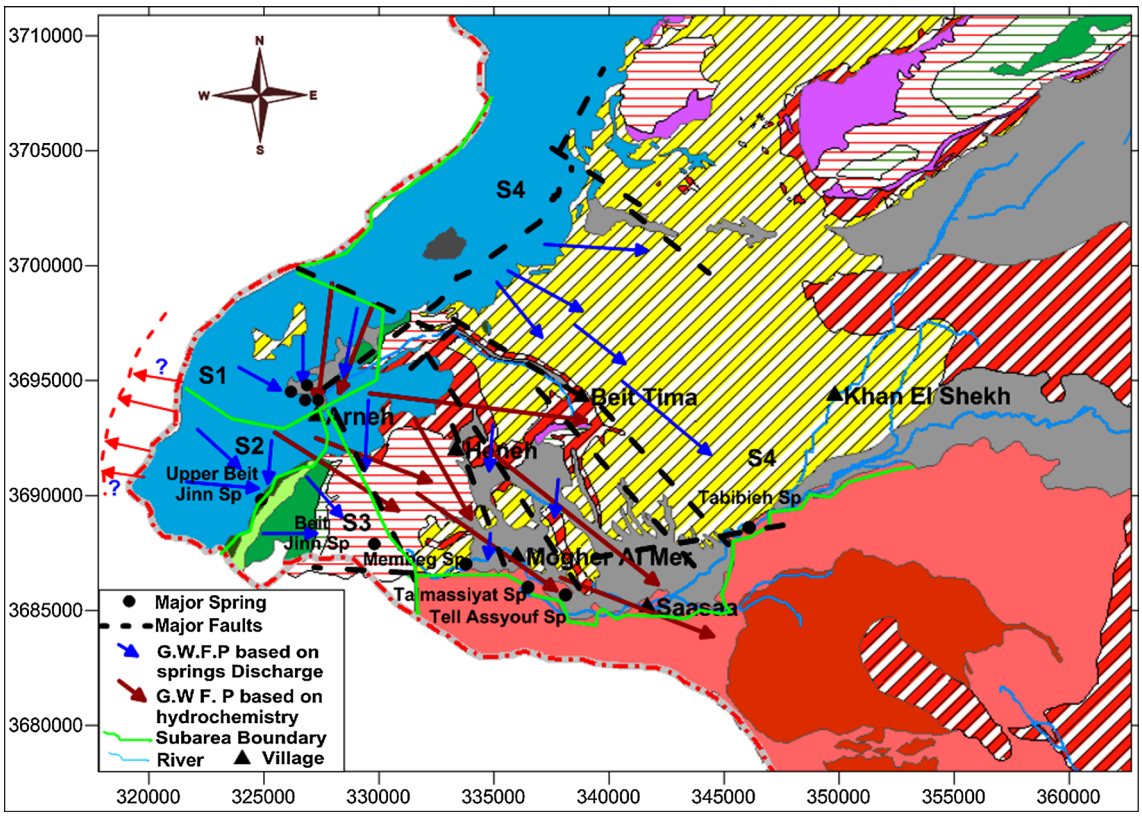

Fig. 12 Schematic groundwater flow pattern based on major springs and hydrochemical tracers and associated hydrogeological subarea

characterising and controlling groundwater flow and its origin. This has allowed to discriminate different main behavioural trends in the groundwater flow pattern. The study area can be divided into two main parts; the south and southeastern parts characterized by a horizontal flow component associated with active interaction between groundwater and hosting rocks, evidenced by water chemistry (water type). The upward leakage seems to play

a significant role in this part. On the other hand, the situation in the western and northwestern parts seems to be a little different. In this part, the karstic feature is well developed, enhancing the infiltration and dissolution mechanisms. Therefore, the vertical flow seems to be a dominant scheme. Consequently, hydrochemical patterns did not give enough evidences for expecting a huge feeding flow from Jurassic aquifers towards the other aquifers. Important anthropogenic influence through infiltration of irrigation water in the plain area has been also detected.

The results show that the hydrochemical evolution is not clear enough to provide an effective approach to delineate the flow pattern indicating that this area is much more dominated by recharge than discharge processes. Thus, this area could be considered as a part of a main intermediate or regional flow system more than a local one. The flow pattern is clear from the potentiometric map but that does not tell the whole story about the groundwater behaviour.

Nevertheless, an additional survey of the aquifer mineralogy, a new sampling for isotopes analyses and age-dating techniques will be carried out to propose a quantitative model of the hydrosystems. This will serve as a tool to understand the behaviour of the aquifer system and its response in term of water recharge/discharge, residence time, and water quality.

References

Aghazadeh N, Mogaddam AA (2011) Investigation of hydrochemical characteristics of groundwater in the Harzandat aquifer, Northwest of Iran. Environ Monit Assess 176:183–195

Al-Charideh A (2011) Environmental isotope study of groundwater discharge from the large karst springs in West Syria: a case study of Figeh and Al-sin springs. Environ Earth Sci 63:1–10

Al-Charideh A (2012a) Geochemical and isotopic characterization of groundwater from shallow and deep limestone aquifers system of Aleppo basin (north Syria). Environ Earth Sci 65:1157–1168

Al-Charideh A (2012b) Recharge rate estimation in the Mountain karst aquifer system of Figeh spring, Syria. Environ Earth Sci 65:1169–1178

Al-Charideh A, Abou-Zakhem B (2009) Geochemical and isotopic characterization of groundwater from the Paleogene limestone aquifer of the Upper Jezireh, Syria. Environ Earth Sci 59:1065–1078

Anastasiadis P (2003) Vulnerability of groundwater to agricultural activities Pollution. In: Proceedings of the 8th international conference on environmental science and technology, Lemnos Island, Greece, 8–10 September Full paper, vol B, pp 24–30

Angelakis AN (2000) Water resources management in SAR, with emphasis on non-conventional sources. FAO RNE, Egypt

Appelo CAJ, Postma D (1993) Geochemistry, groundwater and pollution. A.A. Balkema, Rotterdam

Appelo CAJ, Postma D (2005) Geochemistry, groundwater and pollution, 2nd edn. Taylor & Francis, Amsterdam

Barbieri P, Adami G, Favretto A, Lutman A, Avoscan W, Reisenhofer E (2001) Robust cluster analysis for detecting physicochemical typologies of freshwater from wells of the plain of Friuli (northeastern Italy). Anal Chim Acta 440:161–170

Barbieri M, Boschetti T, Petitta M, Tallini M (2005) Stable isotope (^{2}H, ^{18}O and $^{87}Sr/^{86}Sr$) and hydrochemistry monitoring for groundwater hydrodynamics analysis in a karst aquifer (Gran Sasso, Central Italy). Appl Geochem 20:2063–2081

Batiot C, Emblanch C, Blavoux B (2003) Carbone organique total (COT) et magnésium (Mg^{+2}): deux traceurs complémentaires du temps de séjour dans l'aquifère karstique Total Organic Carbon (TOC) and magnesium (Mg^{+2}): two complementary tracers of residence time in karstic systems. CR Geosci 335(2):205–214

Bicalho CC, Batiot-Guilhe C, Seidel JL, Exter SV, Jourde H (2012) Geochemical evidence of water source characterization and hydrodynamic responses in a karst aquifer. J Hydrol 450–451:206–218

Burdon DJ, Safadi C (1964) The karst groundwater of Syria. J Hydrol 2:324–347

Capaccioni B, Didero M, Paletta C, Salvadori P (2001) Hydrochemistry of groundwater from carbonate formation with basal gypsiferous layers. J Hydrol 253:14–26

Deutsch WJ (1997) Groundwater geochemistry: fundamentals and application to contamination. CRC Press, Boca Raton

Domenico PA, Schwartz FW (1990) Physical and chemical hydrogeology. Wiley, New York, p 824

Drever JI (1988) The geochemistry of natural waters. Prentice-Hall, Upper Saddle River

Dubertret L (1932) L'Hydrologie et aperçu sur l'Hydrographie de la Syrie et du Liban dans leurs relations avec la géologie. Rev Géogr Phys Géol Dynamique, TVI fas.4

Edmunds WM, Smedley PL (2000) Residence time indicators in groundwater: the East Midlands Triassic sandstone aquifer. Appl Geochem 15(6):737–752

Edmunds WM, Ma JZ, Aeschbach-Hertig W, Kipfer R, Darbyshire DPF (2006) Groundwater recharge history and hydrogeochemical evolution in the Minqin Basin, North West China. Appl Geochem 21:2148–2170

European Commission (1995) COST Action 65: hydrogeological aspects of groundwater protection in karstic areas. Final report. EUR 16457, Brussels

Fairchild IJ, Borsato A, Tooth AF, Frisia S, Hawkesworth CJ, Huang Y, McDermott F, Spiro B (2000) Controls on trace element (Sr-Mg) compositions of carbonate cave waters: implications for speleothem climatic records. Chem Geol 166(3–4):255–269

FAO (1993) Integrated rural water management. In: Proceedings of the technical consultation on integrated water management, Rome, Italy

Flakova R (1998) Formation and changes of groundwater chemical composition of the Western Carpathian carbonate systems. ACTA Geologica Universitatis Comenianae Nr. 53. Bratislava, Slovakia, pp 5–25

Folch A, Mencio A, Puig R, Soler A, Mas-Pla J (2011) Groundwater development effects on different scale hydrogeological systems using head, hydrochemical and isotopic data and implications for water resources management: the Selva basin (NE Spain). J Hydrol 403:83–102

Freeze RA, Cherry JA (1979) Groundwater. Prentice-Hall, Englewood Cliffs

Guendouz A, Moulla AS, Edmunds WM, Zouari K, Shand P, Mamou A (2003) Hydrogeochemical and isotopic evolution of water in the Complexe Terminal aquifer in the Algerian Sahara. Hydrogeol J 11:483–495

Guler C, Thyne GD (2004a) Delineation of hydrochemical facies distribution in a regional groundwater system by means of fuzzy c-means clustering. Water Resour Res 40:1–11

Guler C, Thyne GD (2004b) Hydrologic and geologic factors controlling surface and groundwater chemistry in Indian Wells-Owens Valley area, southeastern California, USA. J Hydrol 285:177–198

Guler C, Thyne GD, McCray JE, Turner KA (2002) Evaluation of graphical and multivariate statistical methods for classification of water chemistry data. Hydrogeology J10:455–474

Han G, Liu C (2004) Water geochemistry controlled by carbonate dissolution: a study of the river waters draining karst-dominated terrain, Guizhou Province, China. Chem Geol 204:1–21

Hem JD (1985) Study and interpretation of the chemical characteristics of natural water, 3rd edn. U.S. Geological Survey, Water Supply Paper 2254

Hsu KJ (1963) Solubility of dolomite and the composition of Florida groundwaters. J Hydrol 1:288–310

Huneau F, Dakoure D, Celle-Jeanton H, Vitvar T, Ito M, Compaore NF, Traore S, Jirakova H, Le Coustumer P (2011) Flow pattern and residence time of groundwater within the south-eastern Taoudeni sedimentary basin (Burkina Faso, Mali). J Hydrol 409:423–439

INECO Studies and Integration Consulting (2009) Institutional framework and decision-making practices for water management in Syria. Towards the development of strategy for water pollution prevention and control in the Barada River Basin, Greater Damascus area. Contract No: INCO-CT-2006-517673

Jianhua S, Qi F, Xiaohu W, Yonghong S, Haiyang X, Zongqiang C (2009) Major ion chemistry of groundwater in the extreme arid region northwest China. Environ Geol 57:1079–1087

JICA (2001) The study of water resources development in the western and central basins in Syrian Arab Republic, phase I, Ministry of Irrigation (MOI) (in Arabic) (unpublished report)

Kattan Z (1997) Environmental isotope study of the major karst springs in Damascus limestone aquifer systems: case of the Figeh and Barada springs. J Hydrol 193:161–182

Kattan Z (2006) Characterization of surface water and groundwater in the Damascus Ghotta basin: hydrochemical and environmental isotopes approaches. Environ Geol 51:173–201

Kortatsi BK (2007) Hydrochemical framework of groundwater in the Ankobra Basin, Ghana. Aquat Geochem 13:41–74

La-Moreaux PE, Hughes TH, Memon BA, Lineback N (1989) Hydrogeologic assessment—Figeh Spring, Damascus, Syria. Environ Geol Water Sci 13(2):73–127

Langmuir D (1971) The geochemistry of some carbonate groundwaters in central Pennsylvania. Geochim Cosmochim Acta 35:1023–1045

Lawrence AR, Gooddy DC, Kanatharana P, Meesilp M, Ramnarong V (2000) Groundwater evolution beneath Hat Yai, a rapidly developing city in Thailand. Hydrogeol J 8:564–575

Li X, Zhang L, Hou X (2008) Use of hydrogeochemistry and environmental isotopes for evaluation of groundwater in Qingshuihe Basin, northwestern China. Hydrogeol J 16:335–348

López-Chicano M, Bouamama M, Vallejos A, Pulido-Bosch A (2001) Factors which determine the hydrogeochemical behaviour of karstic springs. A case study from the Betic Cordilleras, Spain. Appl Geochem 16(9–10):1179–1192

Ma JZ, Edmunds WM (2006) Groundwater and lake evolution in the Badain Jaran desert ecosystem, Inner Mongolia. Hydrogeol J 14:1231–1243

Ma JZ, Wang XS, Edmunds WM (2005) The characteristics of groundwater resources and their changes under the impacts of human activity in the arid Northwest China, a case study of the Shiyang River Basin. J Arid Environ 61:277–295

Mahlknecht J, Gárfias-Solis J, Aravena R, Tesch R (2006) Geochemical and isotopic investigations on groundwater residence time and flow in the Independence Basin, Mexico. J Hydrol 324:283–300

McMahon PB, Böhlke JK, Christenson SC (2004) Geochemistry, radiocarbon ages, and paleorecharge conditions along a transect in the central High Plains aquifer, southwestern Kansas, USA. Appl Geochem 19(11):1655–1686

Meslmani Y, Wardeh M F (2010) Strategy and action plan for adaptation to climate change in Syria, (INC-SY_ Strategy & NAPA-En). Ministry of State for Environment Affairs (MSEA)/ United Nations Development Programme (UNDP) Damascus, Syria

MOI (2005) Annual water resources report of Barada and Awaj Basin, Damascus, Syria (in Arabic) (unpublished report)

Moral F, Cruz-Sanjulián JJ, Olías M (2008) Geochemical evolution of groundwater in the carbonate aquifers of Sierra de Segura (Betic Cordillera, southern Spain). J Hydrol 360:281–296

Mourad KA, Berndtsson R (2011) Syrian water resources between the present and the future. Air Soil Water Res 4:93–100. doi:10.4137/ASWR.S8076

Palmer PC, Gannett MW, Stephen R, Hinkle SR (2007) Isotopic characterization of three groundwater recharge sources and inferences for selected aquifers in the upper Klamath Basin of Oregon and California, USA. J Hydrol 336:17–29

Parkhurst DL, Appelo CAJ (1999) PHREEQC for windows version 1.4.07. A hydrogeochemical transport model. U.S. Geological Survey Software

Plummer LN (1977) Defining reactions and mass transfer in part of the Floridan aquifer. Water Resour Res 13(5):801–812

Plummer LN, Wigley TML, Parkhurst DL (1978) The kinetics of calcite dissolution in CO_2 water systems at 5–60 °C and 0.0–1.0 atm CO_2. Am J Sci 278(2):179–216

Plummer LN, Busby JF, Lee RW, Hanshaw BB (1990) Geochemical modeling of the Madison aquifer in parts of Montana, Wyoming, and south Dakota. Water Resour Res 26(9):1981–2014

Ponikarov VO (1967) The geology of Syria, explanatory notes on the map of Syria, Scale 1:500,000. Part II. Mineral deposits and underground water resources. Technoexport, Moscow

Rakhmatullaev S, Huneau F, Kazbekov J, Le Coustumer P, Jumanov J, El Oifi B, Motelica-Heino M, Hrkal Z (2010) Groundwater resources and management in the Amu Darya River Basin (Central Asia). Environ Earth Sci 59:1183–1193

Rakhmatullaev S, Huneau F, Kazbekov J, Celle-Jeanton H, Motelica-Heino M, Le Coustumer P, Jumanov J (2012) Groundwater resources of Uzbekistan: an environmental and operational overview. Cent Eur J Geosci 4:67–80

RDAWSA (2006) Interim report—hydrogeological study of Mougher El Mer Area, Damascus Rural water and sanitation project

Schoeller H (1956) Géochimie des eaux souterraines. Application aux eaux des gisements de petrole. Soc Ed Technip, Paris

Selkhozpromexport (1986) Water resources use in Barada and Awaj Basins for irrigation of crops, Syria Arab Republic. USSR, Ministry of Land Reclamation and Water Management, Moscow

Stadler S, Geyh MA, Ploethner D, Koeniger P (2012) The deep Cretaceous aquifer in the Aleppo and Steppe basins of Syria: assessment of the meteoric origin and geographic source of the groundwater. Hydrogeol J 20:1007–1026. doi:10.1007/s10040-012-0862-2

Stuyfzand PJ (1989) A new hydrochemical classification of water type. IAHS Red Books 182:89–98

Suk H, Lee K–K (1999) Characterization of a ground water hydrochemical system through multivariate analysis: clustering into groundwater zones. Ground Water 37:358–366

Vengosh A, Rosenthal E (1994) Saline groundwater in Israel: its bearing on the water crisis in the country. J Hydrol 156:389–430

Wen X, Wu Y, Zhang Y, Liu F (2005) Hydrochemical characteristics and salinity of groundwater in the Ejina basin, northwestern China. Environ Geol 48:665–675

Wolfart R (1964) Hydrogeology of the Damascus Basin (southwest-Syria). IAHS Red Books 64:402–413